Robotic Artificial Muscles: Current Progress and Future Perspectives

Jun Zhang, Jun Sheng, Ciarán T. O'Neill, Conor J. Walsh, Robert J. Wood, Jee-Hwan Ryu, Jaydev P. Desai, and Michael C. Yip

***Abstract*—Robotic artificial muscles are a subset of artificial muscles that are capable of producing biologically inspired motions useful for robot systems - i.e., large power-to-weight ratios, inherent compliance, and large range of motions. These actuators, ranging from shape memory alloys to dielectric elastomers, are increasingly popular for biomimetic robots as they may operate without using complex linkage designs or other cumbersome mechanisms. Recent achievements in fabrication, modeling, and control methods have significantly contributed to their potential utilization in a wide range of applications. However, no survey paper has gone into depth regarding considerations pertaining to their selection, design, and usage in generating biomimetic motions. This paper will discuss important characteristics and considerations in the selection, design, and implementation of various prominent and unique robotic artificial muscles for biomimetic robots, and provide perspectives on next-generation muscle-powered robots.**

I. INTRODUCTION

Artificial muscles are broadly defined as the materials and devices that can change their shapes under external chemical or physical stimuli [1]–[3]. A subset of artificial muscles, defined as robotic artificial muscles, are actuators that conform to biologically inspired manners to generate work. These actuators, ranging from shape memory alloys (SMA) to dielectric elastomers, offer many advantages over conventional rigid actuators (e.g., electric motors) – i.e., high power-to-weight ratio, high force-to-weight ratio, inherent compliance, and all without complex linkages [4]–[9]. Robotic artificial muscles have shown strong potential as driving mechanisms for novel robotic applications such as robot manipulators and grippers, biomimetic robots, robotic prosthetics and exoskeletons, medical robots, soft robots, and many others [10]–[16].

Since the last decade, the utilization of robotic artificial muscles has grown substantially in part due to the significant advancements in the fabrication, modeling, and control methods for such systems. However, no survey paper has gone into details about the selection, design, and usage considerations of various prominent robotic artificial muscles for generating biomimetic motions. Past survey papers have either covered the broad topic of general artificial muscles [1] or focused on a few particular aspects of a specific robotic artificial muscle. For example, [2], [3] focused on the working mechanisms of artificial muscles, [17], [18] focused on aerospace applications and soft robots composed of SMA actuators, and [4] focused on wearable robotic orthoses applications using robotic artificial muscles. [19], [20] reviewed the models of SMA and McKibben actuators, [18] discussed the designs and applications of SMA actuators, [21] reviewed the technology, applications, and challenges of dielectric elastomer actuators (DEAs), and [22] surveyed the design, modeling, and control of manipulation using pneumatic actuators, [23] surveyed the actuation and sensing techniques to realize untethered soft robots, and [24] focused on intrinsically soft artificial materials for small-scale robots.

In this paper, we provide perspectives on important considerations of selection, design, and usage of robotic artificial muscles for biomimetic robots, and discuss the challenges and prospects of future research. The following robotic artificial muscles are covered in depth in this paper: piezoelectric actuators, electroactive polymer (EAP) actuators, which includes DEAs and ionic polymer-metal composites (IPMC) actuators, SMA and shape memory polymer (SMP) actuators, soft fluidic actuators, twisted string actuators (TSAs), and super-coiled polymer (SCP) actuators. Other artificial muscles that have been adopted for robotic applications are briefly discussed but not a focus of this review.

This paper is organized as follows. Section II provides an overview of the working mechanisms and properties of robotic artificial muscles. Section III summarizes the existing studies on the fabrication, modeling, and control of robotic artificial muscles, and discusses the design principles and practical considerations. Section IV highlights the wide range of applications of robotic artificial muscles. Finally, we conclude the paper by discussing the current limitations and challenges of robotic artificial muscles and the prospects on next-generation muscle-powered robots.

II. ROBOTIC ARTIFICIAL MUSCLES

In this section, the working mechanisms and properties of popular robotic artificial muscles are presented. To ensure that we compare all robotic artificial muscles on the same metrics, the following properties are given special considerations: power density, bandwidth, strain, stress, linearity, and energy efficiency. The definitions of the metrics are provided as follows [3], [25], [26]:

This work was supported in part by the National Science Foundation under Grant ECCS-1139773, Grant ECCS-0547131, Grant DGE-0802267, and Grant CMMI-1301243.

Jun Zhang is with the Department of Mechanical Engineering, University of Nevada, Reno, NV 89557, USA (email: jun@unr.edu).

Jun Sheng and Jaydev P. Desai are with the Wallace H. Coulter Department of Biomedical Engineering, Georgia Institute of Technology, Atlanta, GA 30332, USA (e-mail: junsheng@gatech.edu; jaydev@gatech.edu).

Jee-Hwan Ryu is with the School of Mechanical Engineering, Korea University of Technology and Education, Cheonan 330-708, South Korea (e-mail: jhryu@koreatech.ac.kr).

Ciarán T. O'Neill, Conor J. Walsh, and Robert J. Wood are with the School of Engineering and Applied Sciences, Harvard University, Cambridge, MA 02138, USA, and the Wyss Institute for Biologically Inspired Engineering, Harvard University, Boston, MA, 02115, USA (email: ciaranoneill@g.harvard.edu; walsh@seas.harvard.edu; rjwood@seas.harvard.edu).

Michael C. Yip is with the Department of Electrical and Computer Engineering, University of California, San Diego, La Jolla, CA 92093, USA (email: yip@ucsd.edu).

- Power density is the output work generated by the artificial muscle upon excitation normalized to its mass and the actuation period.
- Bandwidth is the maximum trackable sinusoidal frequency of the output amplitude generated by the artificial muscles.
- Strain is the percentage change in length upon excitation normalized to the initial length of the artificial muscle.
- Stress is the generated force artificial muscle upon excitation normalized to its initial cross-sectional area.
- Linearity is the accuracy of a linear model in characterizing or predicting the artificial muscle performance.
- Efficiency is the ratio of output power of the artificial muscle over the input power.

The properties of several popular robotic artificial muscles are displayed in a concise graph in Fig. 1. The values are obtained based on the reported numbers in the existing literature. In particular, the strain is the percentage change of the actuator length normalized to the initial length, regardless of the different motion amplification strategies or actuator configurations. The linearity is obtained by subtracting the root mean square (RMS) error percentage of linear models in characterizing or predicting the artificial muscle performance from 100%. Artificial muscles with less pronounced nonlinearities has higher values of the linearity metric closer to 100%.

While different artificial muscles may have strengths and weaknesses in different property areas, a combination of properties within which they perform well is what give rise to their biomimetic behaviors. The majority of the robotic artificial muscles discussed in this paper are about the actuator materials, but the soft fluidic actuators, TSAs, and SCP actuators work with additional transmission mechanisms. The soft fluidic actuators work under different air pressure controlled by pumps, TSAs work when the strings are twisted with electric motors, and SCP actuators work due to the thermal expansion property and actuator geometric configuration. For these actuators, the overall actuator system is considered for the performance metrics, such as the strain and efficiency. For the other actuators, only the actuator materials are used to compute the performance metrics. Another key characteristic considered is the form factor, which dictates the achievable muscle deformations that can be generated and therefore the scope of suitable use cases. The form factor and types of achievable motions are provided in Fig. 2. Other properties such as voltage requirement, fabrication requirement, and biodegradability, are also discussed.

We summarize the existing studies on the fabrication, modeling, and control of robotic artificial muscles, and discuss the design principles and practical considerations. The existing modeling approaches can often be categorized into phenomenology-based and physics-based, depending on whether the experimental measurement or physical analysis is utilized. Various feedforward and feedback control approaches have been realized to achieve desired performances. The design is often an iterative process – the actuator configuration is first computed based on the desired performance. The preliminary design is then tested and adjusted until the desired performance requirements are met.

A. *Piezoelectric Actuators*

1) Mechanism and Property: Piezoelectric actuators can produce tension or compression in thickness direction under electric fields [52]. When subjected to an electric field, piezoelectric actuators exhibit the converse piezoelectric effect [53]. This effect creates mechanical stress within the microscopic structural lattice of the piezoelectric material, and the produced stress can be translated into displacement or force change [54]. The working mechanism can be briefly described as follows: under no electric field, the cubic unit cells of the material deform into structurally and electrically asymmetric tetragonal unit cells, resulting in a random polarization [53]. Under a strong electric field, the polarization of the domains is forced to align with the applied electric field [55]. This poling process causes an overall deformation or displacement of the material [39], [53], as shown in Fig. 2(a). Lead zirconate titanate (PZT) is the most popular piezoelectric material, and different types and ranges of motion can be realized [56].

The advantages of piezoelectric actuators are high speed, high stress, high energy efficiency, and high positioning precision [53]. Bandwidth can typically be tuned over a wide range. For cyclic operation at hundreds of hertz (Hz), this can lead to power densities that rival or exceed skeletal muscle and come close to macro-scale electromagnetic motors [27]. Piezoelectric actuators can generate high stress up to 110 MPa [15]. The efficiency of a single crystal piezoelectric can reach as high as 90% [18]. Past studies have demonstrated that piezoelectric actuators could generate ultra-high positioning precision up to the sub-nanometer level [57]. The limitations in using piezoelectric actuators are the high voltage, low robustness, low strain, and relatively low power density. The required electric field is typically on the order of 1 MV/m. With a material thicknesses of approximately 100 μm, the required operating voltage will be as high as 100 V. Piezoceramic materials are generally brittle and exhibit a small fracture toughness. The displacement of piezoelectric actuators is often as small as 0.1% [28] and therefore are mostly useful for microstrain motions unless various linkage amplification methods are used. Peak reported power densities are on the order of 0.17 W/g [58], [59].

2) Fabrication: Stacks and bending actuators are created through adhesive lamination [58] while others are created through high-temperature reduction [60]. Fabrication techniques for microelectromechanical systems, such as etching, deposition, and micromachining, are often employed [59]. Many different materials have been successfully employed to fabricate piezoelectric actuators. The materials can be categorized into two groups, one is piezoelectric ceramic materials, and the other is single crystal materials. Popular material options include common polycrystalline ceramics, such as PZT-5A and PZT-5H, and single crystal materials, such as PZN-PT and PMN-PT [61].

3) Modeling: The existing studies of modeling piezoelectric actuators can be classified into three groups: microscopic models, macroscopic models, and hybrid models [53]. The microscopic models and hybrid models often utilize finite element methods and are complicated in derivation and com-

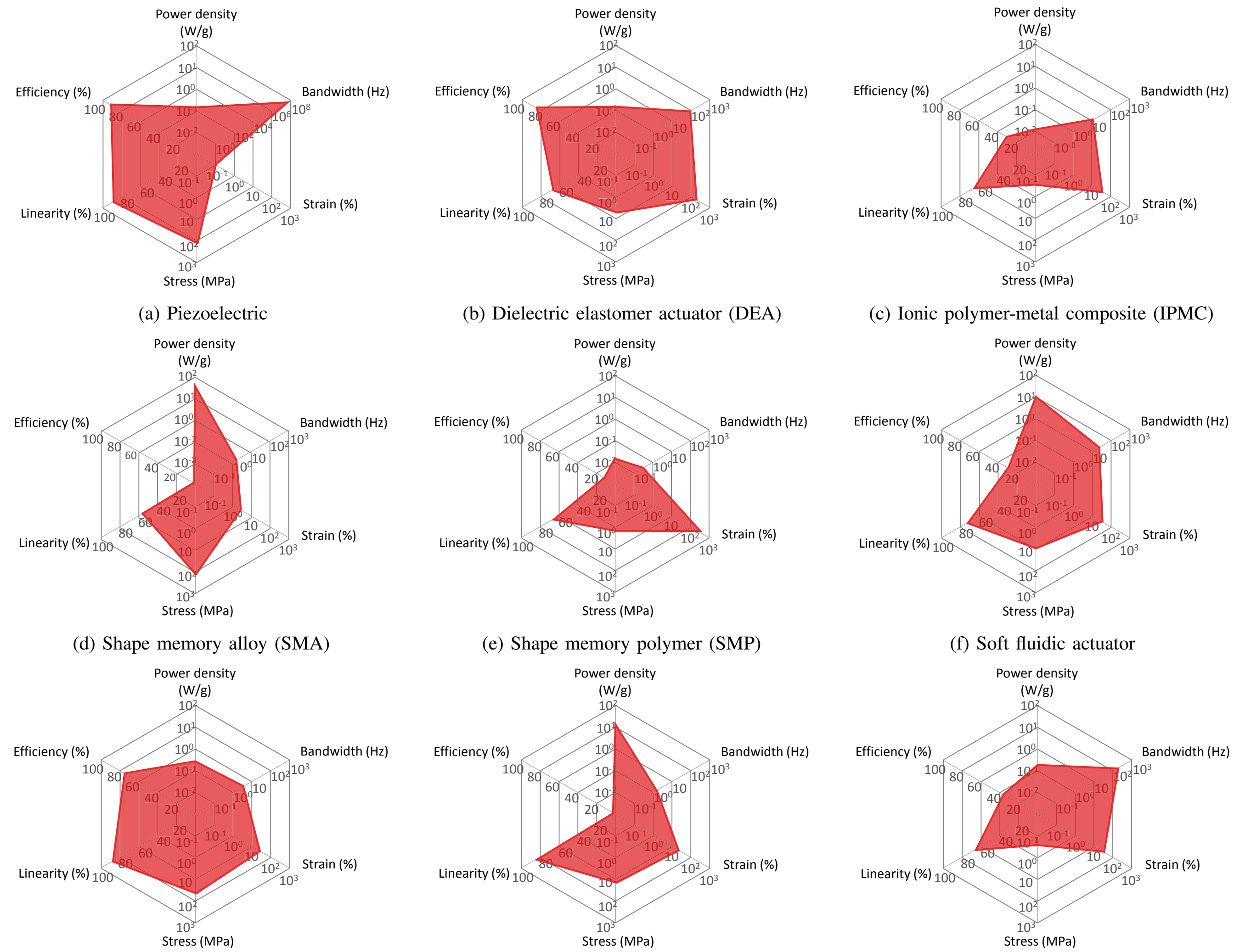

(a) Piezoelectric (b) Dielectric elastomer actuator (DEA) (c) Ionic polymer-metal composite (IPMC)

(d) Shape memory alloy (SMA) (e) Shape memory polymer (SMP) (f) Soft fluidic actuator

(g) Twisted string actuator (TSA) (h) Super-coiled polymer (SCP) (i) Skeletal muscle

Fig. 1. An overall comparison of robotic artificial muscles and skeletal muscles in terms of their power density, bandwidth, strain, stress, linearity, and energy efficiency. This figure should be used as a high-level comparison between actuators, keeping in mind that variations on individual actuators may shift their characteristic charts slightly. For example, (a) piezoelectric actuators have the highest bandwidth (note the scale difference) and efficiency [27], but exhibit low strain and low power density [28]. (b) DEAs produce large strain, reasonably high bandwidth, and high efficiency, but require high voltage [29]. (c) IPMC actuators require low working voltage and can work in aquatic environment, but have low power density and stress [30]. (d) SMA actuators have the highest power density and stress [31], but also high nonlinearity and low efficiency (lower than 1.3%) [18], (e) SMP actuators can produce very large strain [29], but can be slow [32]. (f) Soft fluidic actuators have high power density and good bandwidth, but the required compressors or air sources reduce the effective power to weight ratio [33], [34]. (g) TSAs are intrinsically compliant with good efficiency, but have limited bandwidth and contraction stroke [35], [36]. (h) SCP actuators demonstrate large actuation range and significant mechanical power, but have limited bandwidth and low efficiency which ranges from 0.71% to 1.32% [37], [38].

putation [55]. The macroscopic model is more popular than the other two approaches. The first macroscopic model for piezoelectric actuator was proposed in [62]. However, the model could not reliably describe system dynamics and nonlinearities include hysteresis, creep, and vibration. To capture the hysteresis, both physics-based models and phenomenological models have been proposed [55]. The physics-based models only work for particular materials [63], and thus their uses are limited. Phenomenological models, such as Preisach model, neural network model, and Prandtl-Ishlinskii model [64], [65], are more widely adopted. To characterize creep, both linear and nonlinear models have been developed [66]. To describe the vibrational dynamics, distributed linear models and lumped linear dynamics models have been proposed [67].

4) Control: To realize position control of piezoelectric actuators, both feedforward control and feedback control have been utilized. Feedforward control is often used to compensate for the nonlinearities and vibrational dynamics [68]. By modeling the inverse mapping of the nonlinear relationship, the inverse model can be used as a feedforward controller [69]. For example, to compensate for hysteresis, a numerical inverse of the Preisach model was proposed [57], and an iterative learning strategy was employed to invert the Preisach model [70]. By inverting the hysteresis and creep, desirable performance was obtained [71], [72].

To improve accuracy and robustness, feedback control can be further employed. Proportional-integral-derivative (PID) controllers are widely adopted mainly due to their simplicity

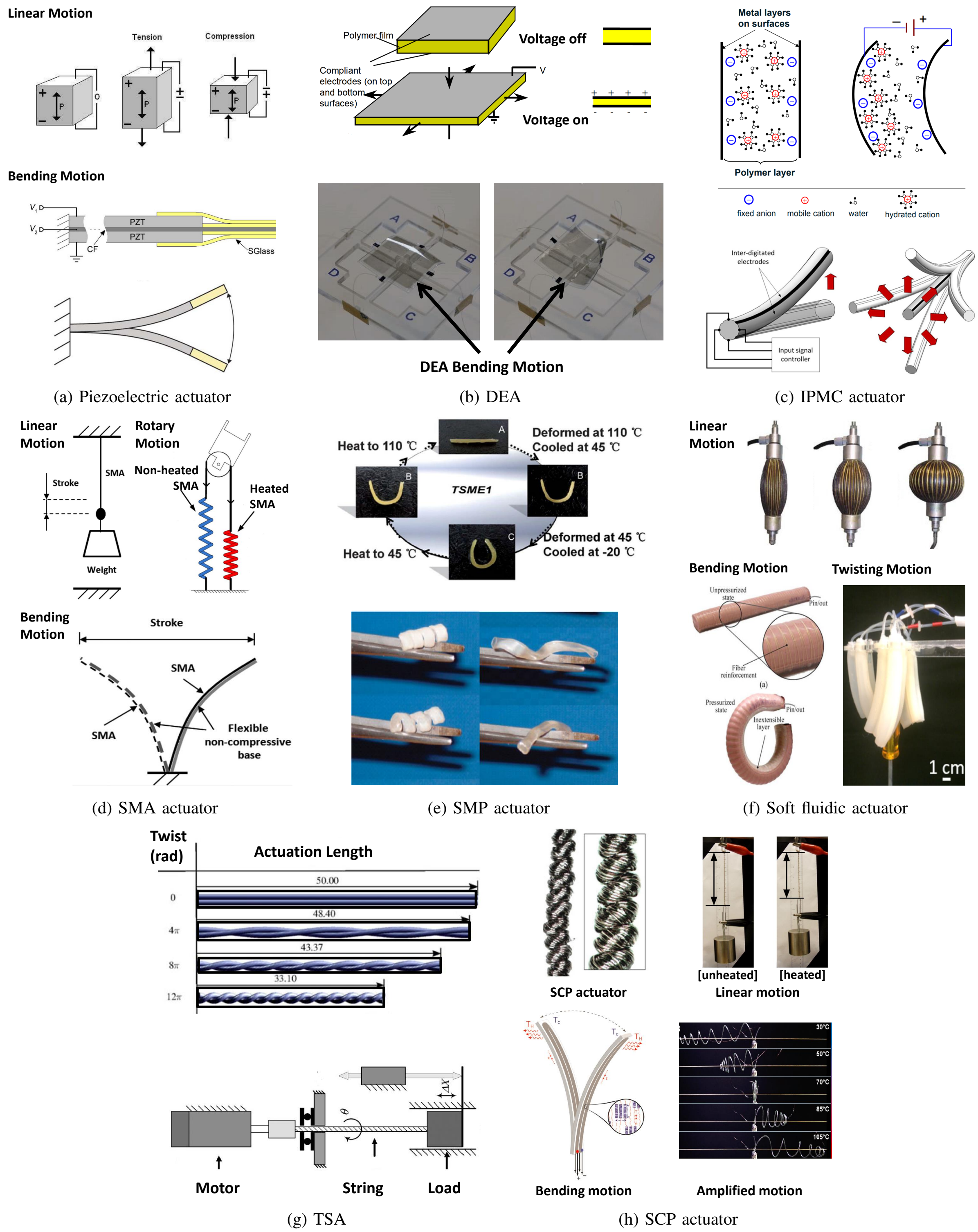

(a) Piezoelectric actuator (b) DEA (c) IPMC actuator

(d) SMA actuator (e) SMP actuator (f) Soft fluidic actuator

(g) TSA (h) SCP actuator

Fig. 2. Working mechanisms and achievable motions of robotic artificial muscles. (a). Piezoelectric actuators can produce motion under electric fields due to the converse piezoelectric effect [39] (top). Bending motions can be realized [12] (bottom). (b). DEA reduces thickness when the differential voltage is applied between the electrodes due to the Coulomb charge attraction effect [40] (top). Bending motion can be realized [9] (bottom). (c). IMPC actuator produces bending motions under an electrical field due to the the fluid-induced swelling force and the electrostatic force [41] (top). Multiple-degree-of-freedom motions can be realized [42]. (d). SMA actuators can produce contractions and elongations under temperature changes due to phase transition. Bending and rotary motions can be realized [11], [31]. (e). SMP actuators can undergo a recoverable deformation and produce complex bending, twisting, folding motions due to shape memory effect [43]. (f). Soft fluidic actuators can produce linear motions under different pressure environments [44]. Bending [45] and twisting motions [46] can be realized. (g). TSA produces linear motions by converting the rotary motion into a linear tensile force [47], [48]. (h). SCP actuators are constructed from twisting polymer fibers or filaments [38]. They can generate linear, bending, and torsional motions due to the thermal expansion property and geometric coil configuration [37], [49]–[51].

and good performance. PID control can eliminate steady-state errors, and are especially effective under static or low-frequency operation [73]. More advanced control methods have also been proposed for high-bandwidth control. Sliding mode control can achieve strong robustness by rejecting the input uncertainties, hysteresis, and other un-modeled disturbances [67], [74]. Robust control can be realized to minimize the effects of disturbances [75].

5) Design: Different design methods for PZTs have been proposed to achieve appreciable motions by motion amplification. One method is to increase the displacement by stacking multiple layers. For example, a 100 μm thick PZT-5H plate with a d_{33} coupling coefficient of 650×10^{-12} m/V operated at 1 MV/m will expand in thickness by approximately 65 nm. 100 layers (for a total thickness of 1 cm) would provide a displacement of 6.5 μm. Other designs can push piezoelectric actuators to generate 5-10% strains. A simple configuration is a bending cantilever. Piezoelectric cantilevers can act as an effective motion amplifying mechanism by converting local strains into bending curvatures, resulting in a large deflection at the distal end of a clamped-free cantilever [76]. However, this method is cumbersome in realization unless for specific applications such as wing flapping, and therefore should be only considered in those limiting cases.

To improve the robustness and reduce the high voltage required for the actuator, there are multiple variations of piezoelectric cantilevers that focus on different manufacturing methods, material combinations, and geometries [77]. For example, LIPCA [78] and THUNDER [79] type actuators are unimorphs that, by virtue of the materials chosen and thermal curing cycle, place the piezoceramic material in compression. This compression enhances the robustness of the actuator.

B. EAP Actuators

1) Mechanism and Property: EAPs are a type of active polymers that can change their shape under electrical stimuli [29], [80]. The most popular types of EAPs are DEAs and IPMC actuators since they exhibit large strain and high bandwidth [81], [82]. DEAs and IPMC actuators will be discussed in detail in this paper.

The working mechanism of DEAs can be described by the Coulomb charge attraction effect. As shown in Fig. 2(b), a DEA consists of a soft elastomeric polymer film, coated on both surfaces by two compliant electrodes [83]. When a differential voltage is applied between the electrodes, a compressive Maxwell stress is produced, causing electrodes to move closer to each other [84]. The resulting film thickness reduction causes the expansion of the material in the other dimensions [85]. Bending motion can also be realized [9], as shown in Fig. 2(b). The advantages of DEAs include large strain, reasonably high bandwidth, good power density, and high efficiency. Up to 200% strain has been demonstrated [29], [86] and DEAs normally work at tens to hundreds of Hz [29]. The power density of a DEA can be 0.2 W/g or lower [3]. The energy efficiency can be as high as 80%-90% [86]. The main disadvantages are the required large voltage and difficulty in producing electrodes. Typical operating electric fields are on the order of 10-100 MV/m, and for common elastomer, this can result in voltages up to 10 kV. Electrodes need to be compatible with high strains, often exceeding 10%.

As shown in Fig. 2(c), an IPMC actuator consists of a membrane sandwiched between two layers of thin metal [41]. Under an electric field, ions and water molecules move to the cathode side, producing bending deformation of the structure toward one of the electrodes [21], [87]. There are two forces which lead to the bending: the fluid-induced swelling force and the electrostatic force due to the imbalanced net charges [41]. Multiple-degree-of-freedom (DoF) motions can be realized [42] (Fig. 2(c)). The main advantages of IMPC actuators include low working voltage (1-5 V), high working frequency (10 Hz and above), large strain (up to 40%), and capability of working in aquatic environment [30], [88]. The main disadvantage of IMPC actuators is their low power density (0.02 W/g) and low stress (up to 0.3 MPa) [15].

2) Fabrication: DEAs consist of elastomers (typically silicones or acrylics) coated with electrodes on two sides. This simple concept has been applied to a host of forms and material combinations that share many characteristics with natural skeletal muscles. There are two main stages during the manufacturing process: coating stage and assembly stage [89]. Small-scale fabrication techniques are available to create dielectric elastomer films, such as spin-coating, spray-coating, and casting [89].

To fabricate IPMC actuators, the first step is to select the base ion exchange polymers and electrodes. The most popular one is Nafion (DuPont) [87]. Platinum is often chosen as the electrode material [88]. By chemically depositing two electrodes on the surface of ion polymers, the IPMC is created [42], [90]. Many techniques have been used to improve the performance of IPMC actuators, such as stiffness tuning [91], patterned electrodes [92], and 3D printing [93].

3) Modeling: Early approaches often approximate the nonlinear and time-dependent viscoelastic properties of DEAs as hyperelastic materials. For example, a physics-based model was proposed for capturing the dynamic response of DEAs where only hyperelastic properties were considered [94]. The nonlinear deformation field theory and thermodynamics were adopted in [95]. Recently, the viscoelastic effect was modeled theoretically [96]. Although analytical models can describe the physical properties of DEAs, they are often computationally expensive. Many numerical models have been developed [97], such as the three-dimensional finite element model to simulate the electromechanical activation process [94].

Similarly, both physics-based models and phenomenology-based models have been proposed for IPMC actuators. By solving the underlying physics, a model incorporating the distributed surface resistance was developed [98]. The electrode surface roughness was modeled physically to estimate the actuator performance [99]. A physics-based model was proposed to describe electrical impedance, charge dynamics, electrochemistry, and cation and water transport process [100]. A circuit model was obtained to characterize the dynamic and nonlinear properties [101]. A data-driven model was obtained by fitting the input-output measurements [102].

4) Control: Different approaches have been presented for controlling DEAs to produce desired motions. Feedforward control of a DEA was realized based on an accurate nonlinear model [103]. Robust control of a DEA was realized to produce guaranteed positioning performance [104] where the DEA was modeled as a linear parameter-varying system. An H_∞ robust controller was derived and implemented for a DEA to track human pulse signals [85].

There are many existing studies on position control and force control for IPMC actuators. To realize position control of an IPMC-actuated robotic finger, a PID controller was successfully employed [105]. Many nonlinear control approaches have also been proposed, such as neural networks and H_∞ controllers [98], [106]. For example, to deal with the dynamics and hysteresis nonlinearity of IPMC actuators, a robust adaptive inverse control approach was adopted [102]. A sliding mode controller was proposed to resist the creep of IPMCs [107]. Force control was realized by feedback control strategies such as time-delay control [108].

5) Design: Design methods for DEAs have been proposed to improve the electrodes quality and reduce the required voltage. To design more physically resilient electrodes that are compatible with the high strains during operation, most DEAs utilize liquid suspensions of conductive particles such as carbon grease. To increase the robustness of the electrodes, many approaches have been proposed including photo-patternable metal-elastomer composite electrodes [109], metal ion implantation [110], physical vapor deposited thin metal films [83], and conductive nanoparticles (i.e., carbon nanotubes) forming a conductive percolation network [9]. To design DEAs that can operate at practical voltages, the dielectric constant is increased, or the thickness of the elastomer layers is decreased. Recently, groups have begun to develop methods to spin cast UV-curable liquid-phase elastomers with thicknesses down to several tens of micrometers [9].

Studies have been conducted on the design of IPMC actuators to obtain a large and complex motion and a large force. First, to generate a large range of motion, the electrode surface of IPMC was designed with multiple sharp tips [111]. A three-fold increase in actuation range was obtained. To design IPMC actuators for complex motions, different fabrication techniques have been proposed [90]. For example, a cylindrical IPMC actuator was manufactured that had two DoFs [42]. By bonding separated IPMC beams with a soft membrane, a hybrid IPMC membrane actuator was capable of generating three-dimensional motions [112]. To design IPMC actuators for a large force, the stiffness of the IMPC actuator was increased by using a thicker layer of Nafion [88].

C. SMA and SMP Actuators

1) Mechanism and Property: The shape memory effect is defined as the property of materials that can change to temporary shapes and then recover their memorized shapes under external stimuli [113]. SMA actuators produce linear contractions and elongations [31], [114]. Other types of motion can also be realized [11], [31], as shown in Fig. 2(d). Nickel Titanium (NiTi) alloys are the most popular kind of SMA actuators [31]. SMP actuators are an emerging class of active polymers that can also undergo a large recoverable deformation [115]. Linear block copolymers and polyesters are commonly used materials [116]. Bending and folding motions can be generated [43], as shown in Fig. 2(e).

Under stimuli, the crystal structures of SMA and SMP go through phase transformations, during which their properties vary with temperature, stress, and strain [117]. At a low temperature, the crystal structure is initially formed in the twinned martensite phase. Upon loading, detwinned martensite crystals form after a small elastic region; upon unloading, the SMA retains the deformed shape. When the deformed SMA is heated, a phase transformation to the austenite phase starts and is accompanied by macroscopic shape recovery. If loading is applied during the austenite phase transformation, a recovery force will be exerted to the load. When an SMA is cooled to low temperature, the reverse phase transformation to the martensite phase starts, while the SMA retains the memorized shape when unloaded. An intermediate R-phase might arise before the martensite phase [118]. A unique situation arises when the finish temperature of the austenite phase transformation is lower than room temperature; in this case, the SMA can recover its memorized shape without thermal activation, which is known as superelasticity.

SMA actuators exhibit high power density and high stress. The power density of NiTi SMA can be up to 50 W/g [119], and its recovery stress is as high as 200 MPa [31]. The main limitations of SMA actuators include small contraction, low bandwidth, low efficiency, and significant hysteresis and creep [120]. The maximum recoverable strain range of NiTi SMA is typically up to 5% [121], and most SMA actuators work at low bandwidths due to the thermal nature of the phase transition (<3 Hz) [18]. These actuators often exhibit significant hysteresis between temperature, strain, and tension force [122]. Due to severe thermal loss, power efficiency is typically lower than 1.3 % [31]. SMPs are biodegradable [18] and can produce high recoverable strains (100%-400%) [123]. The main challenges include low recovery stress (1-3 MPa) and low speeds (1s to several minutes). The recovery stresses range from 1-3 MPa, and the recovery response time ranges from 1s to several minutes [32].

2) Fabrication: Most of the off-the-shelf SMA and SMP actuators are commercially available in a variety of geometric forms. Miga Motor and Dynalloy are the two major companies supplying SMA actuated products. Several SMPs have been commercialized in large scales such as polystyrene (Veriflex, Verilyte, Cornerstone Research Group, Inc.) and and epoxy based SMP (TEMBO, Composite Technology Development, Inc.) [124]. To obtain a customized shape memory or transformation temperatures, an already trained SMA or SMP can be re-annealed in the desired shape or an as-drawn material can be fixed in the desired shape and thermally treated in an oven or using a laser [125], [126].

3) Modeling: Phenomenological models have been utilized widely. For example, the Tanaka model [127] uses internal variables to describe thermoplastic phase transformation. Liang and Rogers proposed a 3D model using cosine evolution functions [128]. Neural network models were trained to obtain a forward or inverse model [129], [130]. Other phenomenological models have been proposed, such as neuro-fuzzy inference system model and Preisach model [122], [131].

Physics-based models have undergone significant development, such as microscopic thermodynamic constitutive models and micro-macro models. Microscopic thermodynamic models describe microstructural features, such as phase nucleation, interface motion, and martensite twin growth, at the lattice or grain-crystal levels [19]. They are mostly developed based on the Ginzburge-Landau theory using a polynomial energy expression or molecular dynamics with Newton's equations [132]. The micro-macro models rely on micromechanics to describe the material behavior at the micro or meso scales [133]. The development of micro-macro models requires the use of observable and internal variables [134].

4) Control: Significant effort has been spent to control SMA and SMP actuators to produce desired strain and force. Feedforward controllers have been realized either to compensate for the nonlinearities of the system or to realize some simple tasks [122], [129]. On-off control has been achieved for SMA actuators for many applications, such as morphing of self-reconfigurable robots [135] and locomotion of worm-like biomimetic robots [136], but there are the limiting cases where a constrained number of control options are used to generate a small subset of achievable behaviors.

Feedback approaches have been realized to achieve accurate performance. By controlling the phase transformation of individual segments of an SMA actuator with temperature feedback, the displacement can be controlled [137]. Position feedback control can directly employ position sensing systems [13], [138], [139] as well as sliding-mode control [129], PID control [140], and variable structure control [130]. By integrating the SMA and SMP models with the system dynamic model, advanced model-based controllers were developed, such as linear-quadratic regulator (LQR) control, H_∞ loop shaping, and model predictive control [130], [141].

5) Design: Design strategies for SMA actuators have been proposed to obtain different types of motion, ranges of motion, force, and bandwidth. Wires, sheets, ribbons, and springs are the most commonly used SMA forms to produce linear, bending, and torsional motions. A pre-tensioned SMA wire can generate linear motions [31]. Bending motion can be realized either by connecting wire actuators between hinged links or connecting pre-tensioned SMA wires or springs between the two ends of a flexible beam structure along its longitude [31]. By winding the threads around a cylinder and contracting the wire SMA actuator, rotary motion can be generated [142]. An antagonistic configuration can be adopted to yield larger range of motions [31]. To increase the force output, one approach is to increases Young's modulus ratio between austenite and martensite phases by adjusting the thermal training conditions [143]. Another way is using a thick SMA actuator or multiple actuators [144]. To improve the actuation speed, thin SMA wires with higher surface-area-to-volume ratios can be used. For SMA sheets, meandering patterns can be cut to maximize the resistance path [135]. When SMAs are subjected to liquid or gas flow, the cooling rate can be enhanced [145].

For SMP actuators, design methods have been studied to change the phase transformations and the transition temperatures [43]. To achieve a reliable phase transition, melting and glass transitions have been explored [146]. Triple- and multiple-phase SMPs have been manufactured, which feature one permanent shape and two or more temporary states [147].

D. Soft Fluidic Actuators

1) Mechanism and Property: There are several varieties of soft fluidic actuators, most notable of which are pneumatically driven. Pneumatic artificial muscles (PAMs) convert energy from compressed air to mechanical motion. They can produce linear motions along their axial directions under different pressure [148], [149], as shown in Fig. 2(f). Different versions of PAMs have been developed, such as the McKibben actuators, Pleated PAMs (PPAMs), vacuum-powered PAMs [33], [44], [150], [151]. Extending, bending, and twisting can be realized [45], [46], [152]–[154]. The ability for PAMs to twist and bend has led to the creation of entirely soft grippers and robotic arms capable of interacting with delicate objects.

The most commonly used PAMs are McKibben actuators, which are constructed by coaxially locating a rubber tube within a woven sheath. The rubber tube creates an air tight bladder while the woven sheath protects the bladder and converts the inflation of the bladder into mechanical work. The woven nature of the sheath results in an axial shortening and radial expansion of the actuator when the internal rubber tube is inflated [33]. PPAMs have a similar working mechanism. As shown in Fig. 2(f) (top), in lieu of an elastic airtight bladder, an inextensible, pleated bladder is used which simply unfolds upon inflation allowing efficient radial expansion towards a spherical end shape, lowering the minimum operating pressure. To negate the effects of friction, discrete aramid fibers are laced between the terminations and located within the pleats. Upon inflation, radial expansion displaces the aramid fibers radially, resulting in contraction [150].

PAMs are compliant and lightweight at the site of actuation and have high power density close to 22 W/g [149]. PAMs may be operated hydraulically with little or no change required in the actuator. Hydraulics can improve the system bandwidth beyond 100 Hz [155] and allow for use in hyperbaric atmospheres such as underwater applications with increased weight and reduced compliance. Commercially available McKibben type PAMs are capable of generating large forces close to 6 kN with strokes typically 25% [33], and high power density closes to 10 W/g [3]. PAMs do suffer a number of limitations. While the actuators may have good power to weight ratios, the compressors or air sources required to generate pressure will reduce the effective power to weight ratio of the final robot, and can limit applications to immobile platforms and some specific designs [156]. The energy efficiency from fluid to mechanical is close to 30% [34], [44]. Due to the hysteresis and compliance, the accurate modeling and control of PAMs is difficult [44].

2) Fabrication: McKibben PAMs are simple to manufacture from inexpensive, commonly available materials while delivering peak forces in an order of magnitude greater than a piston of equivalent diameter. McKibben PAMs are constructed of an internal bladder sheathed in a woven braid which acts as the force transmitting element. This braid is typically constructed of aramid fibers, and terminations are attached at either end to constrain radial expansion and couple to external structures. The angle of the weave (relative to the long axis) of the braid changes upon inflation [157]. By varying the starting angles of helical fibers wrapped around the bladder, different motions can be obtained [152]. To fabricate PPAMs, an inextensible, pleated bladder and discrete aramid fibers are used [150].

3) Modeling: The governing equations of the pneumatic actuators have been well explored and validated based on the physical analysis [157]. The force generated by the McKibben PAM is dependent on the angle of the braid weave, the resting diameter, and the contraction ratio of the actuator. The force-displacement curve of a PPAM is similar to that of a McKibben actuator and is related to the actuator initial length and the number of fibers [150]. The maximum contraction length of PPAMs is determined by the slenderness ratio of the actuator [157]. The effects of other actuator configurations are further considered. For example, Connolly, et al. investigated the effects of weave angles in the braids of McKibben type fiber reinforced PAMs [152]. A broader approach to the modeling of dual fiber and fiber reinforced PAMs, covering all possible fiber angles, was undertaken in [158].

Many phenomenology-based approaches have been proposed to characterize the performance of PAMs. The relative motion of the inner bladder and the woven braid generates friction and hysteresis to the force-displacement cycle of the McKibben actuator. To model the friction, an approach is presented by incorporating a hysteresis function into the new modified LuGre model [159]. The hysteresis is typically on the order of 5-7%. The pressure – length hysteresis of a pneumatic actuator system was modeled by a series of Prandtl-Ishlinskii models [160], and the experiment was focused on isobaric cases. In [161], a Maxwell-slip model was proposed as a lumped-parametric model. The virgin curve equation was adopted to describe the friction force.

4) Control: Control of pneumatic actuators is an active research area to obtain desired performances, such as position, force, and impedance. Feedforward control has been realized. For example, by compensating for the friction, a two-staged feedforward force controller was demonstrated [162]. Through inverse dynamics modeling, a fuzzy inverse dynamics controller was realized for trajectory tracking of pneumatic systems [163]; however, the sole use of these non-feedback control mechanisms is not common as they are susceptible to disturbances, creep, and other external effects.

Feedback control is preferred for pneumatic actuators. Some classical approaches, such as PID controllers, have been adopted. In [164], a cascaded proportional-integral (PI) and PID controller was adopted to control the curvature of a soft robot driven by fluidic cylinders. A nonlinear PID control approach was synthesized that could handle the hysteresis of pneumatic actuators [165]. Advanced control methods have been implemented for improved performance. For example, a new backstepping-sliding mode force-stiffness controller was realized for pneumatic cylinders [166]. A sample-based second order sliding mode controller was realized to reduce chattering effect [167]. A sliding-mode control scheme based on an averaged continuous-input model of the discontinuous-input open-loop system was derived to control the position of a pneumatic actuator [168].

5) Design: A number of linear PAMs have been developed which depart from the norms set by McKibbens and PPAMs. Work by Yang, et al. [151] has resulted in the development of vacuum PAMs. These vacuum-actuated muscle-inspired pneumatic structures (VAMPS) consist of a number of interacting elastic beams and cavities sealed within a thin elastomeric membrane. With the application of vacuum, the cavities collapse, causing the actuator to contract. By casting VAMPS from elastomers of differing stiffness, the generated force can be tuned [150]. Recent work by Hawkes, et al. [169] has led to the creation of PAMs capable of 300% strains that operate in an inverted manner to traditional PAMs. Obiajulu, et al. developed methods to achieve greater contractions and forces, and faster responses from a fully soft McKibben PAM [170]. Flat or zero volume PAMs have been developed [171].

Many design strategies have been proposed for pneumatic actuators to obtain composite motions [172], [173]. These actuators may generate greater bending by wrapping them with inextensible fibers to prevent radial expansion. Work by Polygerinos, et al. [45] into modeling the trajectory of bending PAMs allowed for accurate predictions of actuator performance. The ability to accurately model the bending of these PAMs has allowed for the automatic design of composite PAMs [174]. Networks of pneumatic actuators (Pneu-net) have been created to allow for composite motions. Pneu-nets consist of a series of channels and chambers inside an elastomer which change shape when inflated. Recently, modified Pneu-net actuators were developed that significantly reduced the required change in volume for actuation [5]. Textile-based PAMs have been developed that are relatively inexpensive to manufacture while being compliant [175].

E. TSAs

1) Mechanism and Property: TSAs can produce linear motions by converting the rotary motion of an electric motor into a linear tensile force [47], [176]. As shown in Fig. 2(g), a TSA usually consists of a string, an electric motor, and a load [48]. The string is connected coaxially to the electric motor acting as a gear. In order for the string to twist and contract, one end must rotate with respect to the other, and one end must translate linearly with respect to the other [177]. Ultra-high-molecular-weight polyethylene (Dyneema and its derivatives) is the most commonly used string material.

The advantages of TSAs are high translational force with low input torque and the mechanically-simple, muscle-like structure [35], [47], [178]. TSAs can be very light weight and low cost and are intrinsically compliant. The efficiency of the twisted string can reach 85%-90% [48]. Considering the efficiency of conventional DC motors, TSA systems have the overall efficiency of 72%-80% and reasonably high power density of 0.5 W/g. They provide a lot of freedom for designers since motor can be placed coaxially with the axis of motion. Furthermore, they can transmit power over distance [178]. However, TSAs also have several disadvantages. Control is challenging due to nonlinear gear ratio (the transmission ratio is reduced in nonlinear fashion as the string is twisted) [47]. The lifetime can be an issue since strings can be torn out as the twisting and untwisting is repeated [36]. TSAs has limited bandwidth and the contraction stroke is normally about 30% of its untwisted length [176].

2) Modeling: The model of a TSA can be obtained by analyzing the cross-section of a string during twisting [47]. When the string is twisted, the amount of the string contraction can be calculated from the unwound geometry of the cylinder. By differentiating the amount of contraction, the relationship between contraction velocity and angular velocity of the motor can be derived. Thus, given the desired contraction velocity, the corresponding motor angular velocity can be obtained. Under a transparent transmission system (i.e., moderate to low gearing at the motor), a torque balance between the required motor torque for a given external axial force can be calculated [48], [176]. The string radius is crucial for the overall accuracy of the mathematical model. The conventional model assumed constant radius, but there were some recent studies investigating the variation in radius as the string was twisted [48]. In general, the radius of the string will increase with twisting, as the resulting helix formed by the coiling string will tend to expand. Conversely, applying large linear load forces will decrease the radius of the string.

3) Control: There have been limited studies on the control of TSAs. Feedback control of the string contraction can be realized by the measurement of contraction with a linear displacement sensor [176]. The controller commands the motor torque to make the measured contraction follow the desired contraction. However, in many cases, installing a rigid sensor is challenging due to the desired flexibility and light weight. To overcome this, a kinetostatic model can be inverted to calculate the desired motor angle [48]. Regulating the motor angle to the desired motor angle allows the desired contraction to be achieved by using simple motor encoder-based feedback control without using an external sensor. However, this method may have limited repeatability and accuracy in long-term operation due to hysteresis, wear, and creep of the strings. Therefore, combining both approaches may compensate their respective drawbacks. Similarly, tension control can be realized [47].

4) Design: The existing work on the design of TSAs is focused on the study of string materials and mechanisms. The performances of different types of strings under different operation conditions have been tested, in terms of precision, maximum contraction, and lifetime. For example, it was found that individual fibers composing non-braided string can be easily torn or damaged during twisting, while braided strings were more robust [48]. The life cycle of the string was measured under different loads [36]. Variable stiffness can be obtained by adopting antagonistic configurations. In [179], a variable stiffness linear joint driven by antagonistic twisted string actuators was proposed. Recently, a dual-mode TSA mechanism was proposed [178], which allowed the speed mode with low contraction force and the force mode with low contraction speed.

F. SCP Actuators

1) Mechanism and Property: SCP actuators are constructed from twisting polymer fibers or filaments such as carbon nanotube yarns, nylon fishing lines, and sewing threads [37], [180]. As shown in Fig. 2(h), they can generate significant straight contractions, which can be explained as follows [37], [38], [181]: Polymer fibers and filaments are composed of flexible polymer chains. Before twisting, these polymer chains are highly oriented in the fiber direction. The polymer chains are forced into helical configurations when the polymer fibers or filaments are twisted. When twisted polymer threads are also coiled, they form a second, macroscopic helical shape. When the coiled threads are heated, both length contraction of the polymer chains and thread diameter expansion cause the threads to untwist. The produced torque of untwisting induces the contraction whereas the configuration amplifies the contraction by orders of magnitude. Bending and torsional motions can also be realized [50], [51].

SCP actuators have demonstrated large actuation range and significant mechanical power. Up to 21% tensile actuations were demonstrated with the non-mandrel-coiled SCP actuators [37], [182]. The twisting SCP actuators using mandrels can produce up to 49% strain [37]. More recently, a spiral SCP actuator demonstrated an astonishing 8,600% stroke [51]. The power density can be as high as 27 W/g [3], [37], [182]. The SCP actuators can work up to 0.3 Hz in standing air, 1 Hz in forced air, and 7.5 Hz in helium [37], [183]. There are some properties that challenge the full utilization of SCP actuators. The largest force of a single SCP actuator is around 1 N, and multiple actuators are required to obtain a larger force [184], [185]. The SCP actuator exhibits friction-induced hysteresis [181], [183], which can cause up to 15% error with a linear model [49]. The power efficiency ranges from 0.71% to 1.32% [37], [38].

2) Fabrication: SCP actuators are manufactured by twisting yarns or polymers threads until coils are formed. Different materials have been used, such as carbon nanotube yarns, fishing lines, sewing threads, and various polymer fibers or filaments [37], [180]. To produce SCP actuators from thin carbon nanotube yarns, symmetrical twist insertion can be used during sheet draw from a forest or into a pre-drawn nanotube sheet suspended between either a forest and one rigid end support or two rigid end supports [180]. To manufacture SCP actuators from threads with larger diameters like fishing lines, a motor is often used for twist insertion [38]. One end of the thread is attached to a motor, and a weight is hung on the other end to keep the thread taut. As the motor spins, the mass is not allowed to rotate, resulting in twists to the thread. SCP actuators can also be made by wrapping highly twisted fibers around a mandrel [37]. After the thread is fully coiled, heat treatment is performed.

3) Modeling: The majority of the reported studies adopted phenomenology-based models due to the simplicity and effectiveness. The first linear model that could capture the thermomechanical and thermoelectric dynamics was proposed in 2015 [183]. The model was fitted with experimental data and could estimate the dynamic properties of the actuator. Coiling and twisting of fiber threads were suggested to introduce friction and hysteresis [181], [183]. The first model that could capture the hysteresis in SCP actuators was proposed in [49]. The proposed model was able to accurately estimate the relationships between contraction and voltage under different loading conditions. A model was further proposed to describe the strain-temperature hysteresis [186].

A few physics-based models of SCP actuators have been proposed. By modeling the micro-, meso-, and macro-scale thermomechanical actuation using helical spring analysis and molecular level chain interaction theory, a multi-scale model was proposed [187]. By approximating the actuator structure as a single-helix, a model was presented to estimate the stroke and torque [188]. The statics and dynamics of the SCP actuator were modeled from first principles [189].

4) Control: Being a recent technology, limited work has been conducted to control SCP actuators. Strain control and force control of SCP actuators were first realized in [183]. A feedforward force controller was realized using a lead compensator. Strain control and force control using PID controllers were similarly realized [184]. A feedforward controller was proposed to control the strain of the SCP actuator by compensating for the hysteresis [49]. The proposed controller was able to drive the actuator to produce specific lengths of contractions under different loading forces. Recently, accurate strain control was demonstrated for an SMA-fishing-line actuator [190]. The strategy combined feedforward control and feedback control to deal with the system hysteresis and dynamics.

5) Design: Different types of motions can be generated from SCP actuators, such as linear, torsional, and bending motions. The most popular usage of SCP actuators is utilizing their linear motions [37]. Torsional actuation could spin a paddle at speeds of more than 100,000 rpm [51]. Bending and multidirectional motions were demonstrated in [50]. To produce a large range of motion of SCP actuators, one approach is to twist and coil the threads with a mandrel – 49% strain was demonstrated [37]. The other approach is to manufacture the actuator with a spiral mold [51]. To obtain a large force, either thicker SCP actuator [191] or multiple actuators in parallel or bundles [37], [185], [192] can be used. Designing SCP actuators with different bandwidths has also been explored. The bandwidth of the actuator is correlated to the ambient environment and convection or conduction conductivity. In [183], [193], the bandwidths in standing water, standing air, and forced air were measured.

G. Others

Other types of artificial muscles, such as hydraulic actuators, magneto-rheological (MR) actuators, series elastic actuators (SEAs), voice coil actuators (VCAs) have also been exploited for robotic applications. These actuators have many of the important properties that are characteristic of artificial muscles but typically falling short in certain areas.

Hydraulic actuators consist of a piston inside a hollow cylinder. An incompressible liquid from a pump moves the piston inside the cylinder to produce linear motion [194]. They have fast responses and very high power-to-size and power-to-weight ratios. Hydraulic actuators have been widely utilized in industrial robot manipulations. Many studies have investigated control of hydraulic actuators [195]. Like PAMs, they rely on an external fluid pump and liquid volumes. They exhibit minimal compliance and are typically limited in application in macro-scale robots and heavy machinery.

MR actuators are a special class of fluids that can change their stress under a magnetic field [196]. The advantages of MR actuators include high torque-to-mass and torque-to-inertia ratios, fast response, and good controllability [197]. Studies have been conducted to model and control the MR actuators considering their magnetic hysteresis [197]. Popular areas of robotic applications include haptics, telerobotics, and human-robot interaction [198]. MR actuators are still in their infancy and therefore have been designed for larger, bulkier degrees of freedom where braking is more important that actuation. Most studies tested on 1 axis only.

Many variations of electromagnetic actuation have been proposed that can produce muscle-like properties, such as linear motions and compliance. SEAs are the widely used partially due to their compliance. SEAs are realized by connecting a spring in series with a stiff actuator [148]. SEAs have been utilized for biomimetic robots, assistive robots [199], and research platforms like the PR2 [200] and the Baxter robot [201]. The advantages of SEAs include shock tolerance, low reflected inertia, and large dynamic range [202]. SEAs tend to be bulky and difficult to implement over many degrees of freedom with fixed passive stiffness. Another type of widely adopted electromagnetic actuation is the VCAs. A VCA consists of two components: the body and the coil. The body consists of a permanent magnet and an iron core that concentrates magnetic flux radially through the coil, perpendicular to its current flow [203]. Under a magnetic field, the Lorentz force is created to produce actuation [204]. VCAs are direct-drive motors and have been successfully adopted in robotic applications that do not require reduction mechanisms [205], [206]. VCAs have simple structure, small volume, low inertia, large strain, and high efficiency [207]. They produce limited stress and do not exhibit inherent compliance [208].

Artificial muscles with different mechanisms are being actively researched, due to their potential in untethered soft robotics [23]. The morphology of these actuators can be modulated by external wireless stimuli, including light, humidity, and magnetic field [209]–[213]. Most of them are comprised of an anisotropic structure, so that different layers contract or expand at different rates upon excitation to realize bending or displacement. The anisotropic structure can be a composite consisting of layers of different thermomechanical properties [209]–[211] or a thin film grown on a substrate by calcination [212]. Hu et al. have shown that a polymer matrix with embedded magnetic micro-particles can morphologically respond to an external magnetic field [213]. These artificial muscles have been demonstrated in small-scale locomotive robots and grippers [210]–[213], but there still remain a lot of challenges in applying them to broader robotics areas, due to the limitations in their working bandwidth, cycle life,

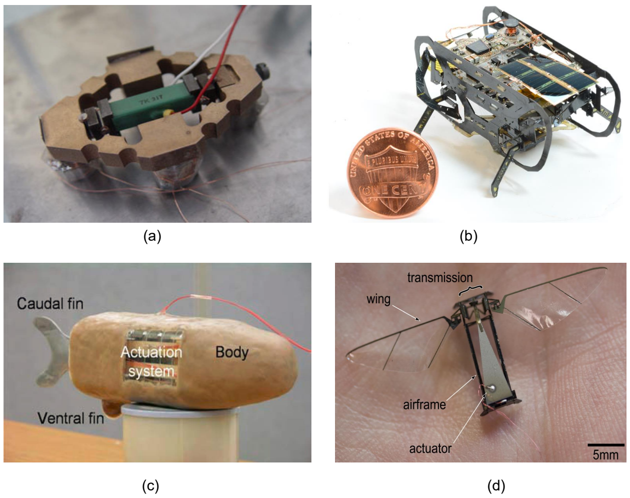

Fig. 3. Robotic applications of piezoelectric actuators: (a) A three-DoF mobile robot [216]. (b) A 2 g hexapod robot as the second generation Harvard Ambulatory MicroRobot [217]. (c) A prototype of a biomimetic fish robot [218]. (d) A prototype of the Harvard RoboBee [12], [27].

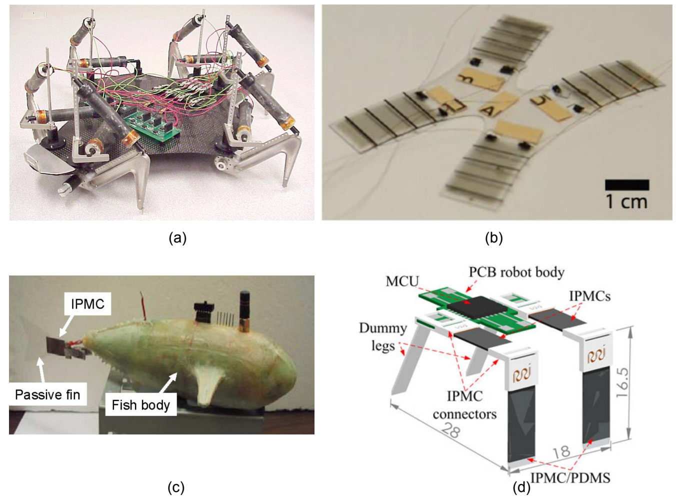

Fig. 4. Robotic applications of DEA and IPMC actuators: (a). An autonomous legged robot actuated by DEAs [40]. (b) A four-legged crawling soft robot based on DEAs [225]. (c) A prototype of a biomimetic fish robot propelled by IPMC actuators [218]. (d) An IPMC-based terrestrial walking robot [82].

scalability, sensor integration, etc.

It is noted that many other types of actuators can produce certain biomimetic properties. For example, ball screw drives, ultrasonic motors, piezo linear actuators, and pneumatic cylinder actuators can all produce linear motions [214], [215].

III. Robotic Applications

In this section, robotic applications of artificial muscles are highlighted.

A. Piezoelectric Actuators

Piezoelectric actuators have been widely used for robotic applications, such as grippers and manipulators, walking robots, swimming robots, and flying robots. Piezoelectric actuators have been used to drive micropositioning stages, micromanipulators, and microgrippers. For example, a three-DoF mobile manipulator driven by piezoelectric stack actuators was developed [216], as shown in Fig. 3(a).

Walking robots actuated by piezoelectric actuators have been developed [219]. Large displacements and forces were demonstrated for piezoelectric actuators-driven inchworm robots [220]. Water strider robots could maintain stability and maneuver on the water surface [14]. A multi-segmented centipede robot and a hexapod robot had good locomotion ability [217], [221], as shown in Fig. 3(b).

Piezoelectric actuators have been utilized to drive swimming robots and flying robots. Piezoceramic actuators were adopted to propel a robotic fish by moving its caudal fins [218], as shown in Fig. 3(c). The tail beat motion was amplified with a linkage system. The Harvard Robobee has been a successful demonstration of utilizing piezoelectric actuation technology for flying robots [12], [27], as shown in Fig. 3(d).

B. EAP Actuators

There have been limited studies on using DEAs for robotic applications. Robotic arms and grippers, biomimetic robots, humanoid robots, and soft robots have been developed and driven by DEAs [222], [223]. The first robotic gripper driven by DEAs was built by the National Aeronautics and Space Administration (NASA) Jet Propulsion Laboratory [224]. The first DEA-driven autonomous legged robot (FLEX) was developed by SRI International (SRI) [40], as shown in Fig. 4(a). A soft actuator based on DEAs was presented [83]. More recently, a DEA-drive, four-legged crawler robot was built that was capable of traveling faster than one body length per second [225], as shown in Fig. 4(b).

A variety of robots have been built with IMPC actuators as the actuation mechanism, such as robotic fishes and vehicles, crawling and walking robots, manipulators and grippers, and soft robots. Being a wet EAP, IPMC actuators are popular for robotic fishes and vehicles [15]. Underwater vehicles and robotic fishes were propelled by vibrating IMPC actuators [92], [226]. The steady-state cruising motion was presented for an IPMC-propelled robotic fish, as shown in Fig. 4(c) [41]. Biomimetic robots such as crawling robots and walking robots have been developed [88], [93]. An IPMC-actuated terrestrial walking robot was developed with two 2-DoF IPMC legs and two dummy legs [82], as shown in Fig. 4(d).

C. SMA and SMP Actuators

SMA actuators have been exploited for a diverse range of robotic applications, such as medical robots, self-reconfigurable robots, biomimetic robots, robotic hands, manipulators, and exoskeletons. SMA actuators have been employed in medical devices to improve the steerability and maneuverability with negligible increase in device volume and complexity [227], showing their usefulness towards for minimally invasive surgery [125], [228], [229] (Fig. 5(a)). Self-reconfigurable robots have been developed and driven by SMA actuators that can change the relative position or orientation [230]. The recent works focus on the development of robotic origamis [135], [139], as shown in Fig. 5(b). Various

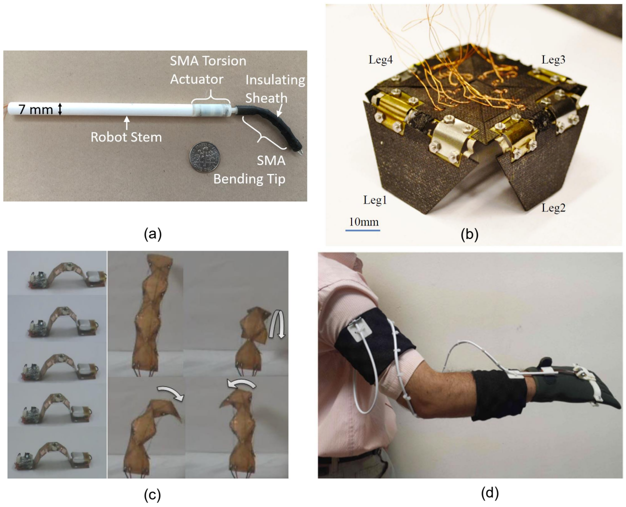

Fig. 5. Robotic applications of SMA and SMP actuators: (a) An SMA-actuated Neurosurgical Intracerebral Hemorrhage Evacuation (NICHE) robot [125]. (b) A four-fold robotic origami with bi-directional actuators formed by antagonistic SMA sheets [139]. (c) A two DoFs inchworm-like crawling robot [136]. (d) A wearable wrist exoskeleton prototype [233].

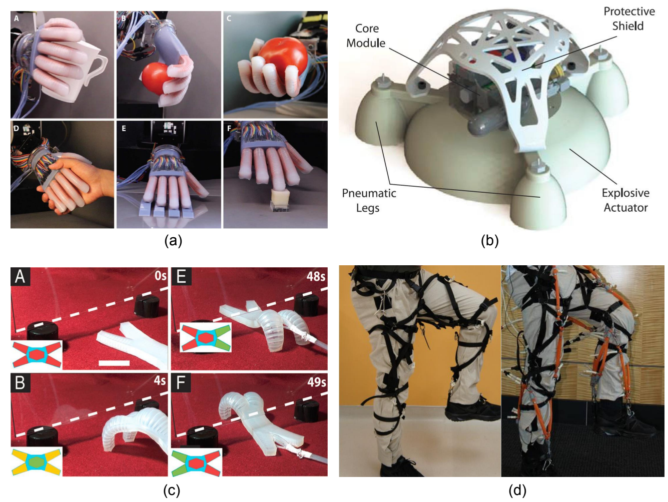

Fig. 6. Robotic applications of soft fluidic actuators: (a) A robotic hand driven by bending Pneu-net type actuators [239]. (b) A 3D-printed, functionally graded soft robot powered by combustion [240]. (c) A pneumatically actuated robot [241]. (d) Robotic soft exosuit driven by McKibben actuators for walking assistance [242].

biomimetic robots have been developed and driven by SMA actuators [231]. As shown in Fig. 5(c), Omegabot can crawl at speed up to 5 mm/s [136]. SMA actuators are widely employed in robotic hands, manipulators [232], and robotic exoskeletons [233], as shown in Fig. 5(d).

The utilization of SMP actuators for robotics is still limited. The main application is for biomedical devices and robotic origamis [13]. For example, an SMP actuator was developed for a biodegradable and elastic suture tool [234]. An SMP-based microactuator was developed to remove blood vessel clots [235]. Exploiting the large recoverable strain, SMPs have been used for stent applications. The cardiovascular stent was preprogrammed to achieve natural deployment [236].

D. Soft Fluidic Actuators

There have been many successful robotic applications utilizing soft fluidic actuators, such as manipulators and grippers, biomimetic robots, and wearable and assistive robots. The use of pneumatic actuators allows for a lightweight and compliant robotic arm which is safe for use in direct contact with humans. Fully soft arms have been realized, such as tentacle continuum robots [237], and arms with multiple distinct inflated segments and joints [238]. To create fully soft robotic arms, soft end effectors typically employ bending Pneu-net type actuators as the fingers of a gripper [239], as shown in Fig. 6(a).

Different biomimetic robots have been developed using pneumatic actuators [152]. Several robots have been developed and driven by Pneu-net actuators to mimic the swimming motion of a range of sea life such as a soft robot mimicking a manta ray [243]. A combustion based jumping robot has been investigated in the search for a greater jump height and horizontal displacement [240], as shown in Fig. 6(b). PAMs were also used in bipedal robot locomotion [244]. Furthermore, the unrestricted rotary motion has been achieved using purely soft actuators by Gong, et al. [245], and fully soft robots have been created to produce quadruped motion [241], as shown in Fig. 6(c).

PAMs have been used in wearable robots. Robotic grip assistance has been achieved using pneumatic actuators [173], [246]. In work [242], a number of McKibben actuators were mounted in parallel to a custom harness to assist with walking, as shown in Fig. 6(d). PAMs have been used to create an ankle assistive device to combat foot drop in patients with neuromuscular disorders [247]. PAMs have also been employed in medical devices for cardiac assistance [248].

E. TSAs

A multi-fingered robotic hand driven by TSAs was developed [249], as shown in Fig. 7(a). Several pinching and grasping tasks were demonstrated. Recently, Jeong et al. developed a robotic hand [178]. Fig. 7(b) shows their anthropomorphic hand, which used active dual-mode twisted actuation for compromising the tradeoff between torque and speed of TSA. The flexibility feature of TSA is very useful for assistive and power augmentation devices. SRI has developed a soft Exo suit, called FlexDrive [250]. Gaponov et al. have proposed a soft portable upper-limb exosuit targeting in-home rehabilitation with shoulder-elbow assistance [251], as shown in Fig. 7(c). TSA is continuously finding new application areas. TSAs can be used to create different tensegrity robots, developed by NASA [252], as shown in Fig 7(d).

F. SCP Actuators

The robotic applications utilizing SCP actuators have been increasing rapidly. The most popular applications are robotic fingers, hands, and arms. The first robotic hand and arm with SCP actuation were demonstrated in [183], as shown in Fig. 8(a). A robotic finger driven by SCP actuators was shown in Fig. 8(b). SCP actuators were utilized for driving

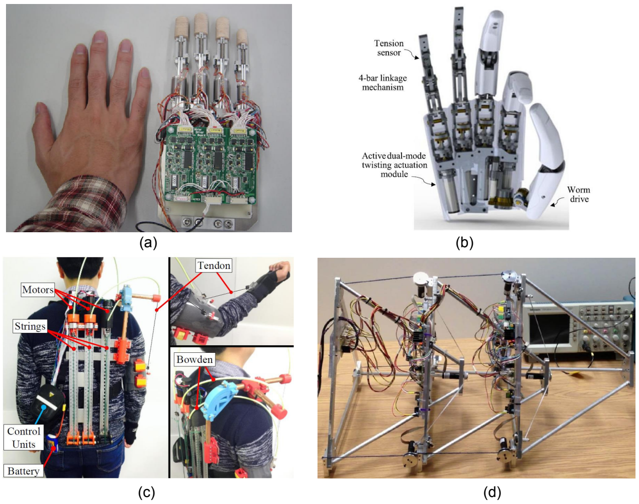

Fig. 7. Robotic applications of TSAs: (a). Lightweight robotic hands [249]. (b). Anthropomorphic robot hand [178]. (c). Auxilio exosuit [251]. (d). A rolling tensegrity robot [252].

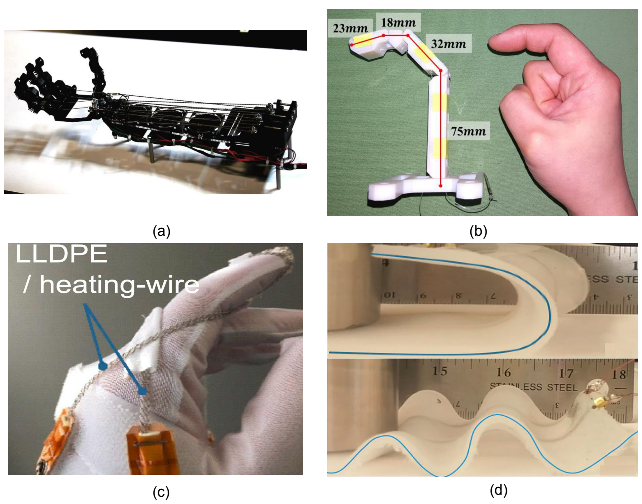

Fig. 8. Robotic applications of SCP actuators: (a) A robot hand [183]. (b) A biomimetic robotic finger [191]. (c) SCP actuators attached to a fabric glove as an assistive device [182]. (d) SCP actuators embedded in soft silicone [254].

robotic fingers and hands in [185], [191], [253]. SCP actuators have been studied for assistive robots. A woven SCP actuator could provide assistance to human finger [182], as shown in Fig. 8(c). The design of a wearable wrist orthosis was demonstrated in [184]. In addition, SCP actuators were employed in soft robotics and underwater robotics. By embedding SCP actuators in the soft silicone skin, soft actuators were created that could produce different undulatory and bending motions [254], [255], as shown in Fig. 8(d).

IV. Future Efforts and Prospects

A. Piezoelectric Actuators

One challenge to adopt piezoelectric actuators for robotic applications is the small range of motion. A simple approach is to stack multiple layers to obtain a multiplied range of motion. However, even using a large number of layers would still produce a small displacement. Other designs such as bending cantilevers and nested-type "flextensional" actuators can produce 5-10% displacement [28], [59], [76]. However, by enlarging the range of motion, the produced force will be decreased. This type of amplification method is also necessary for other actuators exhibiting low strain that are used for applications requiring moderate to large range of motion.

Creating actuators that are robust to damage is also challenging. Piezoelectric materials are generally brittle. Although multiple variations on piezoelectric cantilevers have been proposed to enhance the robustness [78], [79], there are studies that demonstrate the stress-dependence of mechanical and piezoelectric properties [256]. While tensile stress increases fragility, it also increases the coupling coefficients, suggesting a tradeoff between the performance and robustness with respect to pre-stress [63].

Another challenge is the difficulty to reconcile the need for high voltages. Piezoelectric actuators are driven at high electric fields (typically on the order of 1 MV/m) to maximize power density. For example, a piezoelectric material with a thickness of approximately 100 μm often requires an operating voltage of 100 V. Due to the high voltage requirement, the usage of the drive circuitry can cause safety, efficiency, and complexity concerns. Multiple commercially-available high voltage power supplies exist. However, given the brittle nature of most piezoelectric actuators, it is important to consider the nature of the drive signal. For example, depending on the loading conditions, if the drive signal contains frequency content near the resonant frequency of the actuator, there is a risk of damage from amplified motion.

B. EAP Actuators

The main challenges of adopting DEAs for robotic applications are the need for pre-stress, difficulty in creating compatible and robust electrodes, and the required high voltage in operation. Firstly, it is difficult to bias the elastomer to produce an appropriate amount of pre-stress to optimize the actuator performance. Although rigid frames and internal reinforcements could be used [86], these strategies often result in cumbersome mechanisms. Secondly, it is difficult to produce robust electrodes that are compatible with the high strains during operation. Most DEAs utilize liquid suspensions of conductive particles such as carbon grease. This could decrease the bandwidth [257]. Studies have been proposed to improve the physical robustness of the electrodes [9], [109], but these strategies would result in extremely thin layers, causing difficulties in impeding the motion of the actuator or adhesion to additional elastomer layers. Thirdly, operating DEAs at practical voltages is challenging. The existing methods are either to increase the dielectric constant or to decrease the layer thickness. Increasing the dielectric constant often involves the tradeoffs of other material properties. Reducing the thickness of the elastomer layers decreases the force output.

The full potential of IPMC actuators is challenged by the limited motion and force outputs, difficulty in modeling and control, and low physical robustness. First, IPMC actuator has a limited range of motion and force [87]. To increase the force output, thicker Nafion film could be adopted; however, the range of motion would be decreased [88]. To generate a large range of motion, a nanostructured electrode surface of IPMC was designed [111]. The fabrication process was complicated. Secondly, the current numerical models cannot accurately capture the complex physical processes, and physical models are focused more on specific aspects [30]. Finally, more work can be done to manufacture stable and robust IMPC actuators by developing novel polymers and fabrication methods and studying different polymer membranes [30].

C. SMA and SMP Actuators

The primary challenges of utilizing SMA actuators are the small range of motion, low frequency, and difficulty in control. Firstly, it is challenging to achieve a large range of motion for most SMA actuators, considering that the recovery strain of SMA wires is less than 5% [31]. SMA springs are capable of producing large displacements, however, there is a trade-off between the range of motion and force output. Although past studies showed using long SMA actuators or multiple short actuators could increase the range of motion [258], the complexity of the system will be increased. Secondly, high-bandwidth control of SMA actuators is still very difficult. Many studies have been conducted to increase the cooling speed [145], [228], [259]. However, it is cumbersome to integrate a forced convection system on an SMA-actuated robotic system. Thirdly, SMA actuators exhibit significant hysteresis among input, strain, and tension, challenging the accurate control of SMA-actuated robots [120]. Although many hysteresis models have been proposed for SMA actuators, the majority of them are challenging to incorporate for control schemes. Studies can be further conducted to pursue accurate and efficient modeling and control methods [260], [261] for SMA-actuated robotic systems.

The major challenges of using SMP actuators are the low mechanical strength, low recovery stress, long response time, and low cycle life. Reinforcing fillers were used to improve the mechanical performance and increase the shape recovery stress [262]; however, adding fillers complicates the shape control [263]. By embedding a porous carbon nanotube sponge within SMPs, the SMP actuator could be efficiently triggered with low electric power input [264]; however, the fabrication process was complicated.

D. Soft Fluidic Actuators

Further research of soft fluidic actuators is required before they are as widely adopted as more traditional actuation methods. Proper control of PAMs is a key challenge, and multifaceted areas are currently being researched by a number of groups. One such facet is the development of soft sensors for use in soft actuators. For the actuator to remain soft and compliant, the stiffness of the sensor must remain comparable to that of the actuator. This requirement has led to the development of soft sensors to measure strain [265], pressure, and other physical phenomena.

The inherent compliance of the pneumatic actuators typically requires active compensation to account for the effects of gravity and forceful interactions with the environment. Without methods of sensing the state of PAMs and effectively modeling these effects, accurate, and repeatable control of PAM powered devices remains difficult. The control of fluid flow and pressure in PAMs is typically achieved using rigid valves located remotely. The physical scale of these valves in addition to their rigidity limits integration into fully soft systems. Micro and mesoscale soft valves have been developed for microfluidic applications using soft lithographic manufacturing methods, though these valves have yet to make their way into more macro-scale applications.

Finally, a fundamental limitation of all pneumatic and hydraulic systems is the fluidic supply. Pumps and compressors are typically employed to generate sufficient fluidic supply. Pneumatic systems may alternatively be powered from cylinders of compressed gas. However, both methods involve the use of rigid components which limit their use in soft robots.

E. TSAs

The full utilization of TSA has several challenges. One of the major challenges is the limited lifetime. The typical lifetime of TSAs is about 20-30 thousand cycles [48]. The currently recorded lifetime is still much shorter than that of conventional transmission systems. Different materials and operating conditions have been investigated [36], but the issues of degradation and creep still need to be addressed.

Another challenge is the discrepancy between the actual dynamic behavior of the TSA and the kinetostatic modeling under different load forces. An effort to consider the external load variation into the contraction model exists [179], but it cannot be generalized to arbitrary strings and TSA configurations. On the other hand, a position sensor can be used for accurate contraction measurement, but flexible position sensor without erasing TSA's benefits is challenging.

A final challenge is that the basic kinetostatic model does not consider external load variation and variable stiffness. Although there were some initial efforts to model the variable stiffness [179], this still remains an open question. Hysteresis and continuous creep of the strings also make it difficult to obtain an accurate model. Lastly, deviations in string behavior produced by twisting during contact with arbitrary surfaces may potentially make position control of TSAs difficult.

F. SCP Actuators

To practically utilize SCP actuators for robotic applications, a major challenge is to obtain large forces. Different strategies have been explored to increase the force output, such as using multiple SCP actuators in parallel [184], [185]; however, estimation of the force output is difficult. Bundled actuators that had a stable structure were proposed to increase the force output [37], but there have been limited studies to examine the force performance [192].

Another challenge is the slow performance. In standing air, SCP actuators operate at 0.3 Hz or below. When SCP actuators are embedded into a silicone elastomer for soft robots, the speed of the SCP actuators is further decreased [254]. Although recent studies have shown promising results of active cooling techniques [38], [193], these techniques are difficult to realize in practical applications.

Furthermore, due to the hysteresis of SCP actuators, accurate modeling and control can be difficult. Most of the existing studies rely on linear approximations [38], [184], which cannot describe the static hysteretic effects and could cause up to 30% strain difference under the same input [49]. A model was proposed to capture and compensate for the voltage – strain hysteresis [49], with the strain – tension force hysteresis approximated as a polynomial term.

V. Conclusion

Overall, robotic artificial muscles offer a balance of actuation performance, power-to-weight ratio, and inherent compliance in muscle-form factors, thus are strongly desirable as biomimetic actuators for various robotic applications. The study and utilization of robotic artificial muscles have grown significantly in the last decade. To achieve the full potential, fundamental studies are still needed to study how to fabricate, model, control, and design artificial muscles to obtain muscle-like properties and achieve muscle-like behaviors. For example, a common challenge faced by the majority of robotics artificial muscles is the fabrication, integration, and calibration of proprioceptive sensors for feedback-controlled actuation [239], [266]–[269]. Soft strain sensors have been developed for robotic manipulators actuated by PAMs, but there often exists a tradeoff between the sensor stretchability and sensitivity [239], [266], [267]. Solving these challenges has the potential of accelerating the quest for human-like and animal-like robotic behaviors and the distribution of robots into the public [270].

References

[1] B. Tondu, "What is an artificial muscle? A systemic approach." *Actuators*, vol. 4, no. 4, p. 336, 2015.

[2] J. D. Madden, N. A. Vandesteeg, P. A. Anquetil, A. Takshi, R. Z. Pytel, S. R. Lafontaine, P. A. Wieringa, and I. W. Hunter, "Artificial muscle technology: Physical principles and naval prospects," *IEEE J. Oceanic Eng.*, vol. 29, no. 3, pp. 706–728, 2004.

[3] S. M. Mirvakili and I. W. Hunter, "Artificial muscles: Mechanisms, applications, and challenges," *Advanced Materials*, vol. 30, no. 6, p. 1704407, 2017.

[4] A. J. Veale and S. Q. Xie, "Towards compliant and wearable robotic orthoses: A review of current and emerging actuator technologies," *Med. Eng. Phys.*, vol. 38, no. 4, pp. 317–325, 2016.

[5] B. Mosadegh, P. Polygerinos, C. Keplinger, S. Wennstedt, R. F. Shepherd, U. Gupta, J. Shim, K. Bertoldi, C. J. Walsh, and G. M. Whitesides, "Pneumatic networks for soft robotics that actuate rapidly," *Adv. Funct. Mater.*, vol. 24, no. 15, pp. 2163–2170, 2014.

[6] H. Rodrigue, W. Wang, M. W. Han, T. J. Y. Kim, and S. H. Ahn, "An overview of shape memory alloy-coupled actuators and robots," *Soft Robot.*, vol. 4, no. 1, pp. 3–15, 2017.

[7] D. Rus and M. T. Tolley, "Design, fabrication and control of soft robots," *Nature*, vol. 521, pp. 467–475, 2015.

[8] C. Laschi, B. Mazzolai, and M. Cianchetti, "Soft robotics: Technologies and systems pushing the boundaries of robot abilities," *Sci. Robot.*, vol. 1, no. 1, 2016.

[9] M. Duduta, R. J. Wood, and D. R. Clarke, "Multilayer dielectric elastomers for fast, programmable actuation without prestretch," *Adv. Mater.*, vol. 28, pp. 8058–8063, 2016.

[10] J.-S. Koh, E. Yang, G.-P. Jung, S.-P. Jung, J. H. Son, S.-I. Lee, P. G. Jablonski, R. J. Wood, H.-Y. Kim, and K.-J. Cho, "Jumping on water: Surface tension-dominated jumping of water striders and robotic insects," *Science*, vol. 349, no. 6247, pp. 517–521, 2015.

[11] M. Ho, Y. Kim, S. S. Cheng, R. Gullapalli, and J. P. Desai, "Design, development, and evaluation of an MRI-guided SMA spring-actuated neurosurgical robot," *Int. J. Robot. Res.*, vol. 34, no. 8, pp. 1147–1163, 2015.

[12] R. J. Wood, "The first takeoff of a biologically inspired at-scale robotic insect," *IEEE Trans. Robot.*, vol. 24, no. 2, pp. 341–347, 2008.

[13] A. Firouzeh, M. Salerno, and J. Paik, "Stiffness control with shape memory polymer in underactuated robotic origamis," *IEEE Trans. Robot.*, vol. 33, no. 4, pp. 765–777, 2017.

[14] Y. S. Song and M. Sitti, "Surface-tension-driven biologically inspired water strider robots: Theory and experiments," *IEEE Trans. Robot.*, vol. 23, no. 3, pp. 578–589, 2007.

[15] W. S. Chu, K. T. Lee, S. H. Song, M. W. Han, J. Y. Lee, H. S. Kim, M. S. Kim, Y. J. Park, K. J. Cho, and S. H. Ahn, "Review of biomimetic underwater robots using smart actuators," *Int. J. Precis. Eng. Manuf.*, vol. 13, no. 7, pp. 1281–1292, 2012.

[16] A. Miriyev, K. Stack, and H. Lipson, "Soft material for soft actuators," *Nature Communications*, vol. 8, no. 596, 2017.

[17] D. J. Hartl and D. C. Lagoudas, "Aerospace applications of shape memory alloys," *Proc. Inst. Mech. Eng. G: J. Aerosp. Eng.*, vol. 221, no. 4, pp. 535–552, 2007.

[18] J. M. Jani, M. Leary, A. Subic, and M. A. Gibson, "A review of shape memory alloy research, applications and opportunities," *Mater. Des.*, vol. 56, pp. 1078–1113, 2014.

[19] C. Cisse, W. Zaki, and T. B. Zineb, "A review of constitutive models and modeling techniques for shape memory alloys," *Int. J. Plasticity*, vol. 76, pp. 244–284, 2016.

[20] B. Tondu, "Modelling of the McKibben artificial muscle: A review," *J. Intell. Mater. Syst. Struct.*, vol. 23, no. 3, pp. 225–253, 2012.

[21] A. O'Halloran, F. O'Malley, and P. McHugh, "A review on dielectric elastomer actuators, technology, applications, and challenges," *J. Appl. Phys.*, vol. 104, no. 7, 2008.

[22] G. J. Laurent and H. Moon, "A survey of non-prehensile pneumatic manipulation surfaces: Principles, models and control," *Intel. Serv. Robot.*, vol. 8, no. 3, pp. 151–163, 2015.

[23] S. I. Rich, R. J. Wood, and C. Majidi, "Untethered soft robotics," *Nature Electronics*, vol. 1, no. 2, p. 102, 2018.

[24] L. Hines, K. Petersen, G. Z. Lum, and M. Sitti, "Soft actuators for small-scale robotics," *Advanced Materials*, vol. 29, no. 13, 2017.

[25] K. Jin, C. Ryeol, and X. Tan, *Biomimetic Robotic Artificial Muscles*. World Scientific Publishing Company, 2013.

[26] J. Pons, *Emerging Actuator Technologies: A Micromechatronic Approach*. Wiley, 2005.

[27] R. J. Wood, B. Finio, M. Karpelson, K. Ma, N. O. Pérez-Arancibia, P. S. Sreetharan, H. Tanaka, and J. P. Whitney, "Progress on "pico" air vehicles," *Springer Tracts in Advanced Robotics*, vol. 100, pp. 3–19, 2017.

[28] J. Ueda, T. W. Secord, and H. H. Asada, "Large effective-strain piezoelectric actuators using nested cellular architecture with exponential strain amplification mechanisms," *IEEE/ASME Trans. Mech.*, vol. 15, no. 5, pp. 770–782, 2010.

[29] R. Pelrine, R. Kornbluh, Q. Pei, J. Joseph, S. Park, T. Shrout, R. H. Baughman, Q. M. Zhang, V. Bharti, X. Zhao, M. Zhenyi, T. Furukawa, N. Seo, E. Smela, O. Inganäs, I. Lundström, E. Smela, N. Gadegaard, T. Otero, H. B. Schreyer, K. Oguro, H. Tamagawa, R. Kornbluh, R. Pelrine, and R. Heydt, "High-speed electrically actuated elastomers with strain greater than 100%," *Science*, vol. 287, no. 5454, pp. 836–9, 2000.

[30] C. Jo, D. Pugal, I.-K. Oh, K. J. Kim, and K. Asaka, "Recent advances in ionic polymer-metal composite actuators and their modeling and applications," *Prog. Polym. Sci.*, vol. 38, no. 7, pp. 1037–1066, 2013.

[31] J. Mohd Jani, M. Leary, and A. Subic, "Designing shape memory alloy linear actuators: A review," *J. Intell. Mater. Syst. Struct.*, p. 1045389X16679296, 2016.

[32] C. Liu, H. Qin, and P. Mather, "Review of progress in shape-memory polymers," *J. Mater. Chem.*, vol. 17, pp. 1543–1558, 2007.

[33] H. A. Baldwin, "Realizable models of muscle function," in *Proc. Rock Biomechanics Symp.*, 1969, p. 139148.

[34] M. A. Meller, J. B. Chipka, M. J. Bryant, and E. Garcia, "Modeling of the energy savings of variable recruitment McKibben muscle bundles," pp. 1–11, 2015.

[35] H. Singh, D. Popov, I. Gaponov, and J.-H. Ryu, "Twisted string-based passively variable transmission: Concept, model, and evaluation," *Mech. Mach. Theory*, vol. 100, pp. 205–221, 2016.

[36] M. Usman, H. Seong, B. Suthar, I. Gaponov, and J. H. Ryu, "A study on life cycle of twisted string actuators: Preliminary results," in *Proc. IEEE/RSJ Int. Conf. Intell. Robot. Syst.*, 2017, pp. 2789–2794.

[37] C. S. Haines, M. D. Lima, N. Li, G. M. Spinks, J. Foroughi, J. D. W. Madden, S. H. Kim, S. Fang, M. Jung de Andrade, F. Göktepe, Ö. Göktepe, S. M. Mirvakili, S. Naficy, X. Lepró, J. Oh, M. E. Kozlov, S. J. Kim, X. Xu, B. J. Swedlove, G. G. Wallace, and R. H. Baughman, "Artificial muscles from fishing line and sewing thread," *Science*, vol. 343, no. 6173, pp. 868–872, 2014.

[38] M. C. Yip and G. Niemeyer, "On the control and properties of supercoiled polymer artificial muscles," *IEEE Trans. Robot.*, vol. 33, no. 3, pp. 689–699, 2017.

[39] W. Cady, *Piezoelectricity: An introduction to the theory and applications of electromechanical phenomena in crystals*. Dover Publications, 1964.

[40] R. Pelrine, R. Kornbluh, Q. Pei, S. Stanford, S. Oh, J. Eckerle, R. Full, M. Rosenthal, and K. Meijer, "Dielectric elastomer artificial muscle actuators: Toward biomimetic motion," in *Proc. SPIE Electroactive Polymer Actuators and Devices*, vol. 4695, 2002.

[41] Z. Chen, S. Shatara, and X. Tan, "Modeling of biomimetic robotic fish propelled by an ionic polymer-metal composite caudal fin," *IEEE/ASME Trans. Mech.*, vol. 15, no. 3, pp. 448–459, 2010.

[42] S. J. Kim, D. Pugal, J. Wong, K. J. Kim, and W. Yim, "A bio-inspired multi degree of freedom actuator based on a novel cylindrical ionic polymermetal composite material," *Robot. Auton. Syst.*, vol. 62, no. 1, pp. 53–60, 2014.

[43] M. D. Hager, S. Bode, C. Weber, and U. S. Schubert, "Shape memory polymers: Past, present and future developments," *Prog. Polym. Sci*, vol. 49, pp. 3–33, 2015.

[44] D. Villegas, M. V. Damme, B. Vanderborght, P. Beyl, and D. Lefeber, "Third-generation pleated pneumatic artificial muscles for robotic applications: Development and comparison with McKibben muscle," *Adv. Robot.*, vol. 26, no. 11-12, pp. 1205–1227, 2012.

[45] P. Polygerinos, Z. Wang, J. T. B. Overvelde, K. C. Galloway, R. J. Wood, K. Bertoldi, and C. J. Walsh, "Modeling of soft fiber-reinforced bending actuators," *IEEE Trans. Robot.*, vol. 31, no. 3, pp. 778–789, 2015.

[46] B. Shih, D. Drotman, C. Christinason, Z. Huo, R. White, H. I. Christensen, and M. T. Tolley, "Custom soft robotic gripper sensor skins for haptic object visualization," in *Proc. IEEE/RSJ Int. Conf. Intell. Robot. Syst.*, 2017, to appear.

[47] G. Palli, C. Natale, C. May, C. Melchiorri, and T. Wurtz, "Modeling and control of the twisted string actuation system," *IEEE/ASME Trans. Mech.*, vol. 18, no. 2, pp. 664–673, 2013.

[48] I. Gaponov, D. Popov, and J. H. Ryu, "Twisted string actuation systems: A study of the mathematical model and a comparison of twisted strings," *IEEE/ASME Trans. Mech.*, vol. 19, no. 4, pp. 1331–1342, 2014.

[49] J. Zhang, K. Iyer, A. Simeonov, and M. C. Yip, "Modeling and inverse compensation of hysteresis in super-coiled polymer artificial muscles," *IEEE Robot. Autom. Lett.*, vol. 2, no. 2, pp. 773–780, 2017.

[50] S. M. Mirvakili and I. W. Hunter, "Multidirectional artificial muscles from nylon," *Adv. Mater.*, vol. 29, no. 4, p. 1604734, 2017.

[51] C. S. Haines, N. Li, G. M. Spinks, A. E. Aliev, J. Di, and R. H. Baughman, "New twist on artificial muscles," *Proc. Natl. Acad. Sci. USA*, vol. 113, pp. 11 709–11 716, 2016.

[52] J. Ueda, J. Schultz, and H. Asada, *Cellular Actuators: Modularity and Variability in Muscle-inspired Actuation*. Elsevier Science, 2017.

[53] J. Y. Peng and X. B. Chen, "A survey of modeling and control of piezoelectric actuators," *Mod. Mech. Eng.*, vol. 3, no. 1, pp. 1–20, 2013.

[54] Z. Chi and Q. Xu, "Recent advances in the control of piezoelectric actuators," *Int. J. Adv. Robot. Syst.*, vol. 11, no. 11, p. 182, 2014.

[55] G. Bertotti and I. Mayergoyz, *The Science of Hysteresis*. Academic, 2006.

[56] N. Wakita, "Stacked type piezoelectric actuator," 1989, US Patent 4,885,498.

[57] G. Song, J. Zhao, X. Zhou, and J. A. D. Abreu-Garcia, "Tracking control of a piezoceramic actuator with hysteresis compensation using inverse Preisach model," *IEEE/ASME Trans. Mech.*, vol. 10, no. 2, pp. 198–209, 2005.

[58] R. Wood, E. Steltz, and R. Fearing, "Optimal energy density piezoelectric bending actuators," *Sensor. Actuat. A Phys.*, vol. 119, no. 2, pp. 476–488, 2005.

[59] P. A. York and R. J. Wood, "A geometrically-amplified in-plane piezoelectric actuator for mesoscale robotic systems," in *Proc. IEEE Int. Conf. Robot. Autom.*, 2017, pp. 1263–1268.

[60] Q. M. Wang and L. E. Cross, "Tip deflection and blocking force of soft PZT-based cantilever RAINBOW actuators," *J. Am. Ceram. Soc.*, vol. 82, no. 1, pp. 103–110, 1999.

[61] X. Jiang, F. Tang, J. T. Wang, and T. P. Chen, "Growth and properties of PMN-PT single crystals," *Physica C*, vol. 364-365, pp. 678–683, 2001.

[62] IEEE, "ANSI/ IEEE Std. 176-1987: IEEE Standard on Piezoelectricity," The Institute of Electrical and Electronics Engineers, New York, 1988.

[63] G. Yang, S.-F. Liu, W. Ren, and B. K. Mukherjee, "Uniaxial stress dependence of the piezoelectric properties of lead zirconate titanate ceramics," *Proc. of SPIE Smart Mater. Struct.*, vol. 3992, pp. 103–113, 2000.

[64] M. A. Janaideh, S. Rakheja, and C. Y. Su, "An analytical generalized Prandtl-Ishlinskii model inversion for hysteresis compensation in micropositioning control," *IEEE/ASME Trans. Mech.*, vol. 16, no. 4, pp. 734–744, 2011.

[65] D. Habineza, M. Rakotondrabe, and Y. L. Gorrec, "Bouc-Wen modeling and feedforward control of multivariable hysteresis in piezoelectric systems: Application to a 3-DoF piezotube scanner," *IEEE Trans. Contr. Syst. T.*, vol. 23, no. 5, pp. 1797–1806, 2015.

[66] G. Y. Gu, L. M. Zhu, C. Y. Su, H. Ding, and S. Fatikow, "Modeling and control of piezo-actuated nanopositioning stages: A survey," *IEEE Trans. Autom. Sci. Eng.*, vol. 13, no. 1, pp. 313–332, 2016.

[67] H. C. Liaw, B. Shirinzadeh, and J. Smith, "Enhanced sliding mode motion tracking control of piezoelectric actuators," *Sensor. Actuat. A Phys.*, vol. 138, no. 1, pp. 194–202, 2007.

[68] Y. F. Liu, J. Li, X. H. Hu, Z. M. Zhang, L. Cheng, Y. Lin, and W. J. Zhang, "Modeling and control of piezoelectric inertia-friction actuators: review and future research directions," *Mechanical Sciences*, vol. 6, no. 2, pp. 95–107, 2015.

[69] Z. Li and J. Shan, "Modeling and inverse compensation for coupled hysteresis in piezo-actuated-perot spectrometer," *IEEE/ASME Trans. Mech.*, vol. 22, no. 4, pp. 1903–1913, 2017.

[70] K. K. Leang and S. Devasia, "Design of hysteresis-compensating iterative learning control for piezo-positioners: Application to atomic force microscopes," *Mechatronics*, vol. 16, no. 3, pp. 141–158, 2006.

[71] P. Krejci and K. Kuhnen, "Inverse control of systems with hysteresis and creep," *IEE Proceedings - Control Theory and Applications*, vol. 148, no. 3, pp. 185–192, 2001.

[72] K. K. Leang and S. Devasia, "Feedback-linearized inverse feedforward for creep, hysteresis, and vibration compensation in AFM piezoactuators," *IEEE Trans. Contr. Syst. T.*, vol. 15, no. 5, pp. 927–935, 2007.

[73] J. F. Cuttino, A. C. Miller, and D. E. Schinstock, "Performance optimization of a fast tool servo for single-point diamond turning machines," *IEEE/ASME Trans. Mech.*, vol. 4, no. 2, pp. 169–179, 1999.

[74] Q. Xu, "Adaptive discrete-time sliding mode impedance control of a piezoelectric microgripper," *IEEE Trans. Robot.*, vol. 29, no. 3, pp. 663–673, 2013.

[75] G. Schitter, P. Menold, H. F. Knapp, F. Allgwer, and A. Stemmer, "High performance feedback for fast scanning atomic force microscopes," *Rev. Sci. Instrum*, vol. 72, no. 8, pp. 3320–3327, 2001.

[76] N. T. Jafferis, M. Lok, N. Winey, G.-Y. Wei, and R. J. Wood, "Multilayer laminated piezoelectric bending actuators: Design and manufacturing for optimum power density and efficiency," *Smart Mater. Struct.*, vol. 25, no. 5, p. 055033, 2016.

[77] N. T. Jafferis, M. J. Smith, and R. J. Wood, "Design and manufacturing rules for maximizing the performance of polycrystalline piezoelectric bending actuators," *Smart Mater. Struct.*, vol. 24, no. 6, p. 065023, 2015.

[78] N. S. Goo, C. Kim, Y.-D. Kwon, and K. J. Yoon, "Behaviors and performance evaluation of a lightweight piezo-composite curved actuator," *J. Intell. Mater. Syst. Struct.*, vol. 12, no. 9, pp. 639–646, 2001.

[79] S. A. Wise, "Displacement properties of RAINBOW and THUNDER piezoelectric actuators," *Sensor. Actuat. A Phys.*, vol. 69, no. 97, pp. 33–38, 1998.

[80] Y. Bar-Cohen, *Electroactive Polymer (EAP) Actuators as Artificial Muscles: Reality, Potential, and Challenges*, ser. Press Monograph Series. Society of Photo Optical, 2004.

[81] Y. Bahramzadeh and M. Shahinpoor, "A review of ionic polymeric soft actuators and sensors," *Soft Robot.*, vol. 1, no. 1, pp. 38–52, 2014.

[82] K. T. Nguyen, S. Y. Ko, J. O. Park, and S. Park, "Terrestrial walking robot with 2-DOF ionic polymer-metal composite (IPMC) legs," *IEEE/ASME Trans. Mech.*, vol. 20, no. 6, pp. 2962–2972, 2015.

[83] M. Cianchetti, V. Mattoli, B. Mazzolai, C. Laschi, and P. Dario, "A new design methodology of electrostrictive actuators for bio-inspired robotics," *Sensor. Actuat. B Chem.*, vol. 142, no. 1, pp. 288–297, 2009.

[84] J. S. Plante and S. Dubowsky, "Large-scale failure modes of dielectric elastomer actuators," *Int. J. Solids Struct.*, vol. 43, no. 25-26, pp. 7727–7751, 2006.

[85] Z. Ye, Z. Chen, R. Asmatulu, and H. Chan, "Robust control of dielectric elastomer diaphragm actuator for human pulse signal tracking," *Smart Mater. Struct.*, vol. 26, no. 8, p. 085043, 2017.

[86] R. Pelrine, R. Kornbluh, and G. Kofod, "High-strain actuator materials based on dielectric elastomers," *Adv. Mater.*, vol. 12, no. 16, pp. 1223–1225, 2000.

[87] B. Bhandari, G.-Y. Lee, and S.-H. Ahn, "A review on IPMC material as actuators and sensors: Fabrications, characteristics and applications," *Int. J. Precis. Eng. Manuf.*, vol. 13, no. 1, pp. 141–163, 2012.

[88] Y. C. Chang and W. J. Kim, "Aquatic ionic-polymer-metal-composite insectile robot with multi-DoF legs," *IEEE/ASME Trans. Mech.*, vol. 18, no. 2, pp. 547–555, 2013.

[89] R. Sarban, R. W. Jones, B. R. MacE, and E. Rustighi, "A tubular dielectric elastomer actuator: Fabrication, characterization and active vibration isolation," *Mech. Syst. Signal Process.*, vol. 25, no. 8, pp. 2879–2891, 2011.

[90] V. Palmre, J. J. Hubbard, M. Fleming, D. Pugal, S. Kim, K. J. Kim, and K. K. Leang, "An IPMC-enabled bio-inspired bending/twisting fin for underwater applications," *Smart Mater. Struct.*, vol. 22, no. 1, p. 014003, 2013.

[91] Z. Chen and X. Tan, "Monolithic fabrication of ionic polymermetal composite actuators capable of complex deformation," *Sensor. Actuat. A Phys.*, vol. 157, no. 2, pp. 246–257, 2010.

[92] J. J. Hubbard, M. Fleming, V. Palmre, D. Pugal, K. J. Kim, and K. K. Leang, "Monolithic IPMC fins for propulsion and maneuvering in bioinspired underwater robotics," *IEEE J. Oceanic Eng.*, vol. 39, no. 3, pp. 540–551, 2014.

[93] J. D. Carrico, K. J. Kim, and K. K. Leang, "3D-printed ionic polymer-metal composite soft crawling robot," in *Proc. IEEE Int. Conf. Robot. Autom.*, 2017, pp. 4313–4320.

[94] M. Wissler and E. Mazza, "Modeling of a pre-strained circular actuator made of dielectric elastomers," *Sensor. Actuat. A Phys.*, vol. 120, no. 1, pp. 184–192, 2005.

[95] T. He, L. Cui, C. Chen, and Z. Suo, "Nonlinear deformation analysis of a dielectric elastomer membranespring system," *Smart Mater. Struct.*, vol. 19, no. 8, p. 085017, 2010.

[96] G. Y. Gu, U. Gupta, J. Zhu, L. M. Zhu, and X. Zhu, "Modeling of viscoelastic electromechanical behavior in a soft dielectric elastomer actuator," *IEEE Trans. Robot.*, 2017, [Online]: Available: http://ieeexplore.ieee.org, DOI: 10.1109/TRO.2017.2706285.

[97] A. Buschel, S. Klinkel, and W. Wagner, "Dielectric elastomers numerical modeling of nonlinear visco-electroelasticity," *Int. J. Numer. Methods Eng.*, vol. 93, no. 8, pp. 834–856, 2013.

[98] Z. Chen and X. Tan, "A control-oriented and physics-based model for ionic polymer–metal composite actuators," *IEEE/ASME Trans. Mech.*, vol. 13, no. 5, pp. 519–529, 2008.

[99] M. Aureli and M. Porfiri, "Effect of electrode surface roughness on the electrical impedance of ionic polymermetal composites," *Smart Mater. Struct.*, vol. 21, no. 10, p. 105030, 2012.

[100] Z. Zhu, L. Chang, T. Horiuchi, K. Takagi, A. Aabloo, and K. Asaka, "Multi-physical model of cation and water transport in ionic polymer-metal composite sensors," *J. Appl. Phys.*, vol. 119, no. 12, p. 124901, 2016.

[101] C. Bonomo, L. Fortuna, P. Giannone, S. Graziani, and S. Strazzeri, "A nonlinear model for ionic polymer metal composites as actuators," *Smart Mater. Struct.*, vol. 16, no. 1, p. 1, 2007.

[102] Z. Sun, L. Hao, W. Chen, Z. Li, and L. Liu, "A novel discrete adaptive sliding-mode-like control method for ionic polymer-metal composite manipulators," *Smart Mater. Struct.*, vol. 22, no. 9, p. 095027, 2013.

[103] G. Y. Gu, U. Gupta, J. Zhu, L. M. Zhu, and X. Y. Zhu, "Feedforward deformation control of a dielectric elastomer actuator based on a nonlinear dynamic model," *Appl. Phys. Lett.*, vol. 107, no. 4, p. 042907, 2015.

[104] G. Rizzello, D. Naso, B. Turchiano, and S. Seelecke, "Robust position control of dielectric elastomer actuators based on LMI optimization," *IEEE Trans. Contr. Syst. T.*, vol. 24, no. 6, pp. 1909–1921, 2016.

[105] C. Gonzalez and R. Lumia, "An IPMC microgripper with integrated actuator and sensing for constant finger-tip displacement," *Smart Mater. Struct.*, vol. 24, no. 5, p. 055011, 2015.

[106] A. Hunt, Z. Chen, X. Tan, and M. Kruusmaa, "An integrated electroactive polymer sensor-actuator: Design, model-based control, and performance characterization," *Smart Mater. Struct.*, vol. 25, no. 3, p. 035016, 2016.

[107] L. Hao, Y. Chen, and Z. Sun, "The sliding mode control for different shapes and dimensions of IPMC on resisting its creep characteristics," *Smart Mater. Struct.*, vol. 24, no. 4, p. 045040, 2015.

[108] M. H. Kim, K. Y. Kim, J. H. Lee, J. Y. Jho, D. M. Kim, K. Rhee, and S. J. Lee, "An experimental study of force control of an IPMC actuated two-link manipulator using time-delay control," *Smart Mater. Struct.*, vol. 25, no. 11, p. 117001, 2016.

[109] M. G. Urdaneta, R. Delille, and E. Smela, "Stretchable electrodes with high conductivity and photo-patternability," *Adv. Mater.*, vol. 19, no. 18, pp. 2629–2633, 2007.

[110] S. Rosset, M. Niklaus, P. Dubois, and H. R. Shea, "Metal ion implantation for the fabrication of stretchable electrodes on elastomers," *Adv. Funct. Mater.*, vol. 19, no. 3, pp. 470–478, 2009.

[111] V. Palmre, D. Pugal, K. J. Kim, K. K. Leang, K. Asaka, and A. Aabloo, "Nanothorn electrodes for ionic polymer-metal composite artificial muscles," *Sci. Rep.*, vol. 4, 2014.

[112] Z. Chen, T. I. Um, and H. Bart-Smith, "A novel fabrication of ionic polymermetal composite membrane actuator capable of 3-dimensional kinematic motions," *Sensor. Actuat. A Phys.*, vol. 168, no. 1, pp. 131–139, 2011.

[113] A. Ölander, "An electrochemical investigation of solid cadmium-gold alloys," *J. Am. Chem. Soc.*, vol. 54, no. 10, pp. 3819–3833, 1932.

[114] S. Seok, C. D. Onal, K. J. Cho, R. J. Wood, D. Rus, and S. Kim, "Meshworm: A peristaltic soft robot with antagonistic nickel titanium coil actuators," *IEEE/ASME Tran. Mech.*, vol. 18, no. 5, pp. 1485–1497, 2013.

[115] L. Hines, V. Arabagi, and M. Sitti, "Shape memory polymer-based flexure stiffness control in a miniature flapping-wing robot," *IEEE Trans. Robot.*, vol. 28, no. 4, pp. 987–990, 2012.

[116] M. Behl and A. Lendlein, "Shape-memory polymers," *Mater. Today*, vol. 10, no. 4, pp. 20–28, 2007.

[117] L. Sun and W. M. Huang, "Nature of the multistage transformation in shape memory alloys upon heating," *Met. Sci. Heat Treat.*, vol. 51, no. 11, pp. 573–578, 2009.

[118] M. Karhu and T. Lindroos, "Long-term behaviour of binary Ti–49.7 Ni (at.%) SMA actuatorsthe fatigue lives and evolution of strains on thermal cycling," *Smart Mater. Struct.*, vol. 19, no. 11, p. 115019, 2010.

[119] I. W. Hunter, J. M. Hollerbach, and J. Ballantyne, "A comparative analysis of actuator technologies for robotics," *Robotics Review*, vol. 2, pp. 299–342, 1991.

[120] J. Zhang, A. Simeonov, and M. C. Yip, "Three-dimensional hysteresis compensation enhances accuracy of robotic artificial muscles," *Smart Mater. Struct.*, vol. 27, no. 3, p. 035002, 2018.

[121] M. Mertmann and G. Vergani, "Design and application of shape memory actuators," *Eur. Phys. J*, vol. 158, no. 1, pp. 221–230, 2008.

[122] J. Zhang and M. C. Yip, "Three-dimensional hysteresis modeling of robotic artificial muscles with application to shape memory alloy actuators," in *Proc. Robotics: Science and Systems XIII*, 2017.

[123] K. Gall, P. Kreiner, D. Turner, and M. Hulse, "Shape-memory polymers for microelectromechanical systems," *J. Microelectromech. Syst.*, vol. 13, no. 3, pp. 472–483, 2004.

[124] H. Meng and G. Li, "A review of stimuli-responsive shape memory polymer composites," *Polymer*, vol. 54, no. 9, pp. 2199–2221, 2013.

[125] E. Ayvali, C.-P. Liang, M. Ho, Y. Chen, and J. P. Desai, "Towards a discretely actuated steerable cannula for diagnostic and therapeutic procedures," *Int. J. Robot. Res.*, vol. 31, no. 5, pp. 588–603, 2012.

[126] J. Sheng and J. P. Desai, "Design, modeling and characterization of a novel meso-scale SMA-actuated torsion actuator," *Smart Mater. Struct.*, vol. 24, no. 10, p. 105005, 2015.

[127] K. Tanaka, "A thermomechanical sketch of shape memory effect: One-dimensional tensile behavior," 1986.

[128] C. Liang and C. A. Rogers, "One-dimensional thermomechanical constitutive relations for shape memory materials," *J. Intell. Mater. Syst. Struct.*, vol. 8, no. 4, pp. 285–302, 1997.

[129] G. Song, V. Chaudhry, and C. Batur, "Precision tracking control of shape memory alloy actuators using neural networks and a sliding-mode based robust controller," *Smart Mater. Struct.*, vol. 12, no. 2, p. 223, 2003.

[130] N. Nikdel, P. Nikdel, M. A. Badamchizadeh, and I. Hassanzadeh, "Using neural network model predictive control for controlling shape memory alloy-based manipulator," *IEEE Trans. Ind. Electron.*, vol. 61, no. 3, pp. 1394–1401, 2014.

[131] A. Kilicarslan, G. Song, and K. Grigoriadis, "Modeling and hysteresis compensation in a thin SMA wire using ANFIS methods," *J. Intell. Mater. Syst. Struct.*, vol. 22, no. 1, pp. 45–57, 2011.

[132] M. I. Baskes, "Modified embedded-atom potentials for cubic materials and impurities," *Phys. Rev. B*, vol. 46, pp. 2727–2742, 1992.

[133] E. Oberaigner, , K. Tanaka, and F. Fischer, "The influence of transformation kinetics on stress-strain relations of shape memory alloys

in thermomechanical processes," *J. Intell. Mater. Syst. Struct.*, vol. 5, no. 4, pp. 474–486, 1994.

[134] T. Mori and K. Tanaka, "Average stress in matrix and average elastic energy of materials with misfitting inclusions," *Acta Metallurgica*, vol. 21, no. 5, pp. 571–574, 1973.

[135] J. K. Paik, E. Hawkes, and R. J. Wood, "A novel low-profile shape memory alloy torsional actuator," *Smart Mater. Struct.*, vol. 19, no. 12, p. 125014, 2010.

[136] J. S. Koh and K. J. Cho, "Omegabot: Biomimetic inchworm robot using SMA coil actuator and smart composite microstructures (SCM)," in *Proc. IEEE Int. Conf. Robot. Biomim.*, 2009, pp. 1154–1159.

[137] B. Selden, K. Cho, and H. H. Asada, "Segmented shape memory alloy actuators using hysteresis loop control," *Smart Mater. Struct.*, vol. 15, no. 2, p. 642, 2006.

[138] J. Sheng and J. P. Desai, "A novel meso-scale SMA-actuated torsion actuator," in *Proc. IEEE/RSJ Int. Conf. Intell. Robot. Syst.*, 2015, pp. 4718–4723.

[139] A. Firouzeh, Y. Sun, H. Lee, and J. Paik, "Sensor and actuator integrated low-profile robotic origami," in *Proc. IEEE/RSJ Int. Conf. Intell. Robot. Syst.*, 2013, pp. 4937–4944.

[140] J. Ko, M. B. Jun, G. Gilardi, E. Haslam, and E. J. Park, "Fuzzy PWM-PID control of cocontracting antagonistic shape memory alloy muscle pairs in an artificial finger," *Mechatronics*, vol. 21, no. 7, pp. 1190–1202, 2011.

[141] J. Jayender, R. V. Patel, S. Nikumb, and M. Ostojic, "Modeling and control of shape memory alloy actuators," *IEEE Trans. Contr. Syst. T.*, vol. 16, no. 2, pp. 279–287, 2008.

[142] J. Sheng, D. Gandhi, R. Gullapalli, J. M. Simard, and J. P. Desai, "Development of a meso-scale SMA-based torsion actuator for image-guided procedures," *IEEE Trans. Robot.*, vol. 33, no. 1, pp. 240–248, 2017.

[143] I. Spinella, G. S. Mammano, and E. Dragoni, "Conceptual design and simulation of a compact shape memory actuator for rotary motion," *J. Mater. Eng. Perform.*, vol. 18, no. 5-6, pp. 638–648, 2009.

[144] K. J. D. Laurentis, A. Fisch, J. Nikitczuk, and C. Mavroidis, "Optimal design of shape memory alloy wire bundle actuators," in *Proc. IEEE Int. Conf. Robot. Autom.*, vol. 3, 2002, pp. 2363–2368.

[145] Y. Kim, S. S. Cheng, A. Ecins, C. Fermüller, K. P. Westlake, and J. P. Desai, "Towards a robotic hand rehabilitation exoskeleton for stroke therapy," in *Proc. ASME Dyn. Syst. Contr. Conf.*, 2014, p. V001T04A006.

[146] J. Hu, Y. Zhu, H. Huang, and J. Lu, "Recent advances in shape-memory polymers: Structure, mechanism, functionality, modeling and applications," *Prog. Polym. Sci*, vol. 37, no. 12, pp. 1720–1763, 2012.

[147] Q. Zhao, M. Behl, and A. Lendlein, "Shape-memory polymers with multiple transitions: Complex actively moving polymers," *Soft Matter*, vol. 9, pp. 1744–1755, 2013.

[148] R. V. Ham, T. G. Sugar, B. Vanderborght, K. W. Hollander, and D. Lefeber, "Compliant actuator designs," *IEEE Robot. Autom. Mag.*, vol. 16, no. 3, pp. 81–94, 2009.

[149] C.-P. Chou and B. Hannaford, "Measurement and modeling of McKibben pneumatic artificial muscles," *IEEE Trans. Robot. Autom.*, vol. 12, no. 1, pp. 90–102, 1996.

[150] F. Daerden, "Conception and realization of pleated pneumatic articial muscles and their use as compliant actuation elements," Master Thesis, Vrije University Brussel, Belgium, 1999.

[151] D. Yang, M. S. Verma, J.-H. So, B. Mosadegh, C. Keplinger, B. Lee, F. Khashai, E. Lossner, Z. Suo, and G. M. Whitesides, "Buckling pneumatic linear actuators inspired by muscle," *Adv. Mater. Technol.*, vol. 1, no. 3, p. 1600055, 2016.

[152] F. Connolly, P. Polygerinos, C. J. Walsh, and K. Bertoldi, "Mechanical programming of soft actuators by varying fiber angle," *Soft Robot.*, vol. 2, no. 1, pp. 26–32, 2015.

[153] D. Holland, E. J. Park, P. Polygerinos, G. J. Bennett, and C. J. Walsh, "The soft robotics toolkit: Shared resources for research and design," *Soft Robotics*, vol. 1, no. 3, pp. 224–230, 2014.

[154] S. Li, D. M. Vogt, D. Rus, and R. J. Wood, "Fluid-driven origami-inspired artificial muscles," *Proc. Natl. Acad. Sci. U.S.A.*, 2017.

[155] K. C. Galloway, K. P. Becker, B. Phillips, J. Kirby, S. Licht, D. Tchernov, R. J. Wood, and D. F. Gruber, "Soft robotic grippers for biological sampling on deep reefs," *Soft Robot.*, vol. 3, no. 1, pp. 23–33, 2016.

[156] M. Wehner, M. T. Tolley, Y. Menguec, Y.-L. Park, A. Mozeika, Y. Ding, C. Onal, R. F. Shepherd, G. M. Whitesides, and R. J. Wood, "Pneumatic energy sources for autonomous and wearable soft robotics," *Soft Robot.*, vol. 1, no. 4, pp. 263–274, 2014.

[157] F. Daerden and D. Lefeber, "Pneumatic artificial muscles: Actuators for robotics and automation," *Eur. J. Mech. Environ. Eng.*, vol. 47, no. 1, pp. 11–21, 2002.

[158] J. Bishop-Moser and S. Kota, "Design and modeling of generalized fiber-reinforced pneumatic soft actuators," *IEEE Trans. Robot.*, vol. 31, no. 3, pp. 536–545, 2015.

[159] X. Tran, H. Dao, and K. Tran, "A new mathematical model of friction for pneumatic cylinders," *Proc. Inst. Mech. Eng. C J. Mech. Eng. Sci.*, vol. 230, no. 14, pp. 2399–2412, 2016.

[160] C.-J. Lin, C.-R. Lin, S.-K. Yu, and C.-T. Chen, "Hysteresis modeling and tracking control for a dual pneumatic artificial muscle system using Prandtl-Ishlinskii model," *Mechatronics*, vol. 28, pp. 35–45, 2015.

[161] T. Vo-Minh, T. Tjahjowidodo, H. Ramon, and H. V. Brussel, "A new approach to modeling hysteresis in a pneumatic artificial muscle using the Maxwell-slip model," *IEEE/ASME Trans. Mech.*, vol. 16, no. 1, pp. 177–186, 2011.

[162] J. Y. Lai, C. H. Menq, and R. Singh, "Accurate position control of a pneumatic actuator," in *Proc. American Control Conf.*, 1989, pp. 1497–1502.

[163] K. Balasubramanian and K. S. Rattan, "Feedforward control of a non-linear pneumatic muscle system using fuzzy logic," in *Proc. IEEE Int. Conf. Fuzzy Systems*, vol. 1, 2003, pp. 272–277.

[164] A. D. Marchese, K. Komorowski, C. D. Onal, and D. Rus, "Design and control of a soft and continuously deformable 2D robotic manipulation system," in *Proc. IEEE Int. Conf. Robot. Autom.*, 2014, pp. 2189–2196.

[165] G. Andrikopoulos, G. Nikolakopoulos, and S. Manesis, "Advanced non-linear PID-based antagonistic control for pneumatic muscle actuators," *IEEE Trans. Ind. Electron.*, vol. 61, no. 12, pp. 6926–6937, 2014.

[166] B. Taheri, D. Case, and E. Richer, "Force and stiffness backstepping-sliding mode controller for pneumatic cylinders," *IEEE/ASME Trans. Mech.*, vol. 19, no. 6, pp. 1799–1809, 2014.

[167] A. Estrada and F. Plestan, "Second order sliding mode output feedback control with switching gains: Application to the control of a pneumatic actuator," *J. Franklin Inst.*, vol. 351, no. 4, pp. 2335–2355, 2014.

[168] S. Hodgson, M. Tavakoli, M. T. Pham, and A. Leleve, "Nonlinear discontinuous dynamics averaging and PWM-based sliding control of solenoid-valve pneumatic actuators," *IEEE/ASME Trans. Mech.*, vol. 20, no. 2, pp. 876–888, 2015.

[169] E. W. Hawkes, D. L. Christensen, and A. M. Okamura, "Design and implementation of a 300% strain soft artificial muscle," in *Proc. IEEE Int. Conf. Robot. Autom.*, 2016, pp. 4022–4029.

[170] S. C. Obiajulu, E. T. Roche, F. A. Pigula, and C. J. Walsh, "Soft pneumatic artificial muscles with low threshold pressures for cardiac compression device," in *Proc. ASME 2013 Int. Des. Eng. Tech. Conf. Comput. Inf. Eng. Conf.*, vol. 3, no. 1, 2013, pp. 1–8.

[171] J. Wirekoh and Y.-L. Park, "Design of flat pneumatic artificial muscles," *Smart Materials and Structures*, vol. 26, no. 3, p. 035009, 2017.

[172] F. Ilievski, A. D. Mazzeo, R. F. Shepherd, X. Chen, and G. M. Whitesides, "Soft robotics for chemists," *Angew. Chemie – Int. Ed.*, vol. 50, no. 8, pp. 1890–1895, 2011.

[173] P. Polygerinos, Z. Wang, K. C. Galloway, R. J. Wood, and C. J. Walsh, "Soft robotic glove for combined assistance and at-home rehabilitation," *Rob. Auton. Syst.*, vol. 73, pp. 135–143, 2015.

[174] F. Connolly, C. J. Walsh, and K. Bertoldi, "Automatic design of fiber-reinforced soft actuators for trajectory matching," *Proc. Natl. Acad. Sci. U.S.A.*, vol. 114, no. 1, pp. 51–56, 2017.

[175] C. T. O'Neill, N. S. Phipps, L. Cappello, S. Paganoni, and C. J. Walsh, "A soft wearable robot for the shoulder: Design, characterization, and preliminary testing," in *Int. Conf. Rehabil. Robot.*, 2017, pp. 1672–1678.

[176] T. Wurtz, C. May, B. Holz, C. Natale, G. Palli, and C. Melchiorri, "The twisted string actuation system: Modeling and control," in *Proc. IEEE/ASME Int. Conf. Adv. Intell. Mech.*, 2010, pp. 1215–1220.

[177] C. May, B. Holz, T. Wurtz, C. Natale, G. Palli, and C. Melchiori, "Twisted string actuation history, principle and performance," in *Workshop on Actuation & Sensing in Robotics*, 2010.

[178] S. H. Jeong, K. S. Kim, and S. Kim, "Designing anthropomorphic robot hand with active dual-mode twisted string actuation mechanism and tiny tension sensors," *IEEE Robot. Autom. Lett.*, vol. 2, no. 3, pp. 1571–1578, 2017.

[179] D. Popov, I. Gaponov, and J. H. Ryu, "Towards variable stiffness control of antagonistic twisted string actuators," in *Proc. IEEE/RSJ Int. Conf. Intell. Robot. Syst.*, 2014, pp. 2789–2794.

[180] M. D. Lima, N. Li, M. Jung de Andrade, S. Fang, J. Oh, G. M. Spinks, M. E. Kozlov, C. S. Haines, D. Suh, J. Foroughi, S. J. Kim, Y. Chen, T. Ware, M. K. Shin, L. D. Machado, A. F. Fonseca, J. D. W. Madden, W. E. Voit, D. S. Galvão, and R. H. Baughman, "Electrically,

chemically, and photonically powered torsional and tensile actuation of hybrid carbon nanotube yarn muscles," *Science*, vol. 338, no. 6109, pp. 928–932, 2012.

[181] J. D. W. Madden and S. Kianzad, "Twisted lines: Artificial muscle and advanced instruments can be formed from nylon threads and fabric." *IEEE Pulse*, vol. 6, no. 1, pp. 32–35, 2015.

[182] M. Hiraoka, K. Nakamura, H. Arase, K. Asai, Y. Kaneko, S. W. John, K. Tagashira, and A. Omote, "Power-efficient low-temperature woven coiled fibre actuator for wearable applications," *Sci. Rep.*, vol. 6, no. 36358, 2016.

[183] M. C. Yip and G. Niemeyer, "High-performance robotic muscles from conductive nylon sewing thread," in *Proc. IEEE Int. Conf. Robot. Autom.*, 2015, pp. 2313–2318.

[184] L. Sutton, H. Moein, A. Rafiee, J. D. W. Madden, and C. Menon, "Design of an assistive wrist orthosis using conductive nylon actuators," in *Proc. of IEEE Inter. Conf. Biomed. Robot. Biomech.*, 2016, pp. 1074–1079.

[185] S. Kianzad, J. D. Pandit, Milind Lewis, A. R. Berlingeri, K. J. Haebler, and J. D. Madden, "Variable stiffness and recruitment using nylon actuators arranged in a pennate configuration," in *Proc. SPIE on Electroactive Polymer Actuators and Devices*, vol. 9430, 2015.

[186] T. A. Luong, S. Seo, J. C. Koo, H. R. Choi, and H. Moon, "Differential hysteresis modeling with adaptive parameter estimation of a super-coiled polymer actuator," in *Proc. Int. Conf. Ubiquitous Robots and Ambient Intelligence*, 2017, pp. 607–612.

[187] Q. Yang and G. Li, "A top-down multi-scale modeling for actuation response of polymeric artificial muscles," *J. Mech. Phy. Solids*, vol. 92, pp. 237–259, 2016.

[188] S. Aziz, S. Naficy, J. Foroughi, H. R. Brown, and G. M. Spinks, "Controlled and scalable torsional actuation of twisted nylon 6 fiber," *J. Polym. Sci. Part B Polym. Phys.*, vol. 54, no. 13, pp. 1278–1286, 2016.

[189] A. Abbas and J. Zhao, "A physics based model for twisted and coiled actuator," in *Proc. IEEE Int. Conf. Robot. Autom.*, 2017, pp. 6121–6126.

[190] C. Xiang, H. Yang, Z. Sun, B. Xue, L. Hao, M. D. A. Rahoman, and S. Davis, "The design, hysteresis modeling and control of a novel SMA-fishing-line actuator," *Smart Mater. Struct.*, vol. 26, no. 3, p. 037004, 2017.

[191] K. H. Cho, M. G. Song, H. Jung, J. Park, H. Moon, J. C. Koo, J. D. Nam, and H. R. Choi, "A robotic finger driven by twisted and coiled polymer actuator," in *Proc. of SPIE Electroactive Polymer Actuators and Devices*, vol. 9798, 2016.

[192] A. Simeonov, T. Henderson, Z. Lan, G. Sundar, A. Factor, J. Zhang, and M. Yip, "Bundled super-coiled polymer artificial muscles: Design, characterization, and modeling," *IEEE Robot. Autom. Lett.*, vol. 3, no. 3, pp. 1671–1678, 2018.

[193] S. Kianzad, "A treatment on highly twisted artificial muscle: thermally driven shape memory alloy and coiled nylon actuators," Master Thesis, The University of British Columbia, Canada, 2016.

[194] C. Guan and S. Pan, "Nonlinear adaptive robust control of single-rod electro-hydraulic actuator with unknown nonlinear parameters," *IEEE Trans. Contr. Syst. T.*, vol. 16, no. 3, pp. 434–445, 2008.

[195] M. R. Sirouspour and S. E. Salcudean, "Nonlinear control of hydraulic robots," *IEEE Trans. Robot. Autom.*, vol. 17, no. 2, pp. 173–182, 2001.

[196] M. Jolly, J. Bender, and J. Carlson, "Properties and applications of commercial magnetorheological fluids," *J. Intell. Mater. Syst. Struct.*, vol. 10, no. 1, pp. 5–13, 1999.

[197] P. Yadmellat and M. R. Kermani, "Adaptive control of a hysteretic magnetorheological robot actuator," *IEEE/ASME Trans. Mech.*, vol. 21, no. 3, pp. 1336–1344, 2016.

[198] T. Kikuchi, K. Otsuki, J. Furusho, H. Abe, J. Noma, M. Naito, and N. Lauzier, "Development of a compact magnetorheological fluid clutch for human-friendly actuator," *Adv. Robot.*, vol. 24, no. 10, pp. 1489–1502, 2010.

[199] D. W. Haldane, M. M. Plecnik, J. K. Yim, and R. S. Fearing, "Robotic vertical jumping agility via series-elastic power modulation," *Sci. Robot.*, vol. 1, no. 1, 2016.

[200] J. Bohren, R. B. Rusu, E. G. Jones, E. Marder-Eppstein, C. Pantofaru, M. Wise, L. Mosenlechner, W. Meeussen, and S. Holzer, "Towards autonomous robotic butlers: Lessons learned with the PR2," in *Proc. IEEE Int. Conf. Robot. Autom.*, 2011, pp. 5568–5575.

[201] E. Guizzo and E. Ackerman, "The rise of the robot worker," *IEEE Spectrum*, vol. 49, no. 10, pp. 34–41, 2012.

[202] D. Kim, Y. Zhao, G. Thomas, B. R. Fernandez, and L. Sentis, "Stabilizing series-elastic point-foot bipeds using whole-body operational space control," *IEEE Trans. Robot.*, vol. 32, no. 6, pp. 1362–1379, 2016.

[203] L. E. Ooi, W.-Q. Ho, and W. M. A. W. M. Ali, "Application of voice coil actuator to the measurement of rubber mounts properties," in *IEEE Int. Conf. Control System, Computing and Engineering*, 2016, pp. 517–521.

[204] A. Okyay, M. B. Khamesee, and K. Erkorkmaz, "Design and optimization of a voice coil actuator for precision motion applications," *IEEE Trans. Magn.*, vol. 51, no. 6, pp. 1–10, 2015.

[205] J. Speich and M. Goldfarb, "A compliant-mechanism-based three degree-of-freedom manipulator for small-scale manipulation," *Robotica*, vol. 18, no. 1, p. 95104, 2000.

[206] Z. Batts, J. Kim, and K. Yamane, "Design of a hopping mechanism using a voice coil actuator: Linear elastic actuator in parallel (LEAP)," in *Proc. IEEE Int. Conf. Robot. Autom.*, 2016, pp. 655–660.

[207] Y. Li, Y. Li, L. Ren, Z. Lin, Q. Wang, Y. Xu, and J. Zou, "Analysis and restraining of eddy current damping effects in rotary voice coil actuators," *IEEE Trans. Energy Conver.*, vol. 32, no. 1, pp. 309–317, 2017.

[208] H. M. Herr and R. D. Kornbluh, "New horizons for orthotic and prosthetic technology: Artificial muscle for ambulation," in *Proc. SPIE: Electroactive Polymer Actuators and Devices*, vol. 5385, 2004, pp. 1–9.

[209] M. Amjadi and M. Sitti, "High-performance multiresponsive paper actuators," *ACS Nano*, vol. 10, no. 11, pp. 10 202–10 210, 2016.

[210] Y. Hu, J. Liu, L. Chang, L. Yang, A. Xu, K. Qi, P. Lu, G. Wu, W. Chen, and Y. Wu, "Electrically and sunlight-driven actuator with versatile biomimetic motions based on rolled carbon nanotube bilayer composite," *Advanced Functional Materials*, vol. 27, no. 44, 2017.

[211] D. Copic and A. J. Hart, "Corrugated paraffin nanocomposite films as large stroke thermal actuators and self-activating thermal interfaces," *ACS Applied Materials & Interfaces*, vol. 7, no. 15, pp. 8218–8224, 2015.

[212] H. Arazoe, D. Miyajima, K. Akaike, F. Araoka, E. Sato, T. Hikima, M. Kawamoto, and T. Aida, "An autonomous actuator driven by fluctuations in ambient humidity," *Nature Materials*, vol. 15, no. 10, p. 1084, 2016.

[213] W. Hu, G. Z. Lum, M. Mastrangeli, and M. Sitti, "Small-scale soft-bodied robot with multimodal locomotion," *Nature*, vol. 554, no. 7690, p. 81, 2018.

[214] M. Gienger, K. Loffler, and F. Pfeiffer, "Towards the design of a biped jogging robot," in *Proc. IEEE Int. Conf. Robot. Autom.*, vol. 4, 2001, pp. 4140–4145.

[215] K. Uchino, *Piezoelectric Actuators and Ultrasonic Motors*, ser. Electronic Materials: Science & Technology. Springer US, 1996.

[216] S. Yan, F. Zhang, Z. Qin, and S. Wen, "A 3-DOFs mobile robot driven by a piezoelectric actuator," *Smart Mater. Struct.*, vol. 15, no. 1, pp. 7–13, 2006.

[217] A. T. Baisch, P. S. Sreetharan, and R. J. Wood, "Biologically-inspired locomotion of a 2 g hexapod robot," in *Proc. IEEE/RSJ Int. Conf. Intell. Robot. Syst.*, 2010, pp. 5360–5365.

[218] S. Heo, T. Wiguna, H. C. Park, and N. S. Goo, "Effect of an artificial caudal fin on the performance of a biomimetic fish robot propelled by piezoelectric actuators," *J. Bionic Eng.*, vol. 4, no. 3, pp. 151–158, 2007.

[219] H. H. Hariri, G. S. Soh, S. Foong, and K. Wood, "Locomotion study of a standing wave driven piezoelectric miniature robot for bi-directional motion," *IEEE Trans. Robot.*, vol. 33, no. 3, pp. 742–747, 2017.

[220] J. Li, R. Sedaghati, J. Dargahi, and D. Waechter, "Design and development of a new piezoelectric linear inchworm," *Mechatronics*, vol. 15, no. 6, pp. 651–681, 2005.

[221] K. L. Hoffman and R. J. Wood, "Myriapod-like ambulation of a segmented microrobot," *Autonomous Robots*, vol. 31, no. 1, p. 103, May 2011.

[222] G.-Y. Gu, J. Zhu, L.-M. Zhu, and X. Zhu, "A survey on dielectric elastomer actuators for soft robots," *Bioinspir. Biomim.*, vol. 12, no. 1, p. 011003, 2017.

[223] T. Li, G. Li, Y. Liang, T. Cheng, J. Dai, X. Yang, B. Liu, Z. Zeng, Z. Huang, Y. Luo, T. Xie, and W. Yang, "Fast-moving soft electronic fish," *Sci. Adv.*, vol. 3, no. 4, 2017.

[224] Y. Bar-Cohen, T. Xue, M. Shahinpoor, J. Simpson, and J. Smith, "Flexible, low-mass robotic arm actuated by electroactive polymers and operated equivalently to human arm and hand," in *Conf. and Exposition/Demonstration on Robotics for Challenging Environments*, 1998.

[225] M. Duduta, D. R. Clarke, and R. J. Wood, "A high speed soft robot based on dielectric elastomer actuators," in *Proc. IEEE Int. Conf. Robot. Autom.*, 2017, pp. 4346–4351.

[226] Z. Ye, P. Hou, and Z. Chen, "2D maneuverable robotic fish propelled by multiple ionic polymer–metal composite artificial fins," *Int. J. Intell. Robot. Appl.*, vol. 1, no. 2, pp. 195–208, 2017.

[227] M. Salerno, K. Zhang, A. Menciassi, and J. S. Dai, "A novel 4-DOF origami grasper with an SMA-actuation system for minimally invasive surgery," *IEEE Trans. Robot.*, vol. 32, no. 3, pp. 484–498, 2016.

[228] S. S. Cheng, Y. Kim, and J. P. Desai, "New actuation mechanism for actively cooled SMA springs in a neurosurgical robot," *IEEE Trans. Robot.*, vol. 33, no. 4, pp. 986–993, 2017.

[229] Y. Kim, S. S. Cheng, M. Diakite, R. P. Gullapalli, J. M. Simard, and J. P. Desai, "Toward the development of a flexible mesoscale MRI-compatible neurosurgical continuum robot," *IEEE Trans. Robot.*, (Accepted for publication); DOI: 10.1109/TRO.2017.2719035.

[230] E. Yoshida, S. Murata, S. Kokaji, A. Kamimura, K. Tomita, and H. Kurokawa, "Get back in shape! SMA self-reconfigurable microrobots," *IEEE Robot. Autom. Mag.*, vol. 9, no. 4, pp. 54–60, 2002.

[231] M. Noh, S. W. Kim, S. An, J. S. Koh, and K. J. Cho, "Flea-inspired catapult mechanism for miniature jumping robots," *IEEE Trans. Robot.*, vol. 28, no. 5, pp. 1007–1018, 2012.

[232] H. Ashrafiuon, M. Eshraghi, and M. H. Elahinia, "Position control of a three-link shape memory alloy actuated robot," *J. Intell. Mater. Syst. Struct.*, vol. 17, no. 5, pp. 381–392, 2006.

[233] A. Villoslada, A. Flores, D. Copaci, D. Blanco, and L. Moreno, "High-displacement flexible shape memory alloy actuator for soft wearable robots," *Robot. Auton. Syst.*, vol. 73, pp. 91–101, 2015.

[234] A. Lendlein and R. Langer, "Biodegradable, elastic shape-memory polymers for potential biomedical applications," *Science*, vol. 296, no. 5573, pp. 1673–1676, 2002.

[235] W. Small, M. F. Metzger, T. S. Wilson, and D. J. Maitland, "Laser-activated shape memory polymer microactuator for thrombus removal following ischemic stroke: Preliminary in vitro analysis," *IEEE J. Sel. Top. Quantum Electron.*, vol. 11, no. 4, pp. 892–901, 2005.

[236] W. Small, IV, P. Singhal, T. S. Wilson, and D. J. Maitland, "Biomedical applications of thermally activated shape memory polymers," *J Mater Chem.*, vol. 20, no. 17, pp. 3356–3366, 2010.

[237] R. V. Martinez, J. L. Branch, C. R. Fish, L. Jin, R. F. Shepherd, R. M. D. Nunes, Z. Suo, and G. M. Whitesides, "Robotic tentacles with three-dimensional mobility based on flexible elastomers," *Adv. Mater.*, vol. 25, no. 2, pp. 205–212, 2013.

[238] S. Sanan, P. S. Lynn, and S. T. Griffith, "Pneumatic torsional actuators for inflatable robots," *ASME. J. Mechanisms Robotics.*, vol. 6, no. 3, 2014.

[239] H. Zhao, K. O'Brien, S. Li, and R. F. Shepherd, "Optoelectronically innervated soft prosthetic hand via stretchable optical waveguides," *Sci. Robot.*, vol. 1, no. 1, 2016.

[240] N. W. Bartlett, M. T. Tolley, J. T. B. Overvelde, J. C. Weaver, B. Mosadegh, K. Bertoldi, G. M. Whitesides, and R. J. Wood, "A 3D-printed, functionally graded soft robot powered by combustion," *Science*, vol. 349, no. 6244, pp. 161–165, 2015.

[241] R. F. Shepherd, F. Ilievski, W. Choi, S. A. Morin, A. A. Stokes, A. D. Mazzeo, X. Chen, M. Wang, and G. M. Whitesides, "Multigait soft robot," *Proc. Natl. Acad. Sci. U.S.A.*, vol. 108, no. 51, pp. 20 400–20 403, 2011.

[242] M. Wehner, B. Quinlivan, P. M. Aubin, E. Martinez-Villalpando, M. Baumann, L. Stirling, K. Holt, R. Wood, and C. Walsh, "A lightweight soft exosuit for gait assistance," in *Proc. IEEE Int. Conf. Robot. Autom.*, 2013, pp. 3362–3369.

[243] K. Suzumori, S. Endo, T. Kanda, N. Kato, and H. Suzuki, "A bending pneumatic rubber actuator realizing soft-bodied manta swimming robot," in *Proc. IEEE Int. Conf. Robot. Autom.*, 2007, pp. 4975–4980.

[244] B. Verrelst, R. V. Ham, B. Vanderborght, F. Daerden, D. Lefeber, and J. Vermeulen, "The pneumatic biped "Lucy" actuated with pleated pneumatic artificial muscles," *Auton. Robots*, vol. 18, no. 2, pp. 201–213, 2005.

[245] X. Gong, K. Yang, J. Xie, Y. Wang, P. Kulkarni, A. S. Hobbs, and A. D. Mazzeo, "Rotary actuators based on pneumatically driven elastomeric structures," *Adv. Mater.*, vol. 28, no. 34, pp. 7533–7538, 2016.

[246] H. K. Yap, P. M. Khin, T. H. Koh, Y. Sun, X. Liang, J. H. Lim, and C. H. Yeow, "A fully fabric-based bidirectional soft robotic glove for assistance and rehabilitation of hand impaired patients," *IEEE Robot. Autom. Lett.*, vol. 2, no. 3, pp. 1383–1390, 2017.

[247] M. Wehner, Y. L. Park, C. Walsh, R. Nagpal, R. J. Wood, T. Moore, and E. Goldfield, "Experimental characterization of components for active soft orthotics," in *Proc. IEEE RAS EMBS Int. Conf. Biomed. Robot. Biomechatronics*, 2012, pp. 1586–1592.

[248] E. T. Roche, M. A. Horvath, I. Wamala, A. Alazmani, S.-E. Song, W. Whyte, Z. Machaidze, C. J. Payne, J. C. Weaver, G. Fishbein, J. Kuebler, N. V. Vasilyev, D. J. Mooney, F. A. Pigula, and C. J. Walsh, "Soft robotic sleeve supports heart function," *Sci. Transl. Med.*, vol. 9, no. 373, 2017.

[249] T. Sonoda and I. Godler, "Multi-fingered robotic hand employing strings transmission named 'twist drive'," in *Proc. IEEE/RSJ Int. Conf. Intell. Robot. Syst.*, 2010, pp. 2527–2528.

[250] M. Stevens and A. S. Kernbaum, "Twisted string actuators for exosuits," in *Proc. IEEE/RSJ Int. Conf. Intell. Robot. Syst., Workshop on Twisted String Actuation: State of the Art, Challenges and New Applications*, 2016.

[251] I. Gaponov, D. Popov, S. J. Lee, and J.-H. Ryu, "Auxilio: A portable cable-driven exosuit for upper extremity assistance," *Int. J. Control Autom. Syst.*, vol. 15, no. 1, pp. 73–84, 2017.

[252] I. W. Park and V. SunSpiral, "Impedance controlled twisted string actuators for tensegrity robots," in *Proc. Int. Conf. Control, Automation and Systems*, 2014, pp. 1331–1338.

[253] L. Wu, M. J. de Andrade, L. K. Saharan, R. S. Rome, R. H. Baughman, and Y. Tadesse, "Compact and low-cost humanoid hand powered by nylon artificial muscles," *Bioinspir. Biomim.*, vol. 12, no. 2, p. 026004, 2017.

[254] Y. Almubarak and Y. Tadesse, "Twisted and coiled polymer (TCP) muscles embedded in silicone elastomer for use in soft robot," *Int. J. Intell. Robot. Appl.*, 2017.

[255] S. K. Rajendran and F. Zhang, "Developing a novel robotic fish with antagonistic artificial muscle actuators," in *Proc. ASME Dyn. Syst. Contr. Conf.*, 2017, p. V001T30A011.

[256] S. W. Meeks and R. W. Timme, "Effects of one-dimensional stress on piezoelectric ceramics," *J. Appl. Phys.*, vol. 46, no. 10, pp. 4334–4338, 1975.

[257] S. Ahmed, Z. Ounaies, and M. Frecker, "Investigating the performance and properties of dielectric elastomer actuators as a potential means to actuate origami structures," *Smart Mater. Struct.*, vol. 23, no. 9, 2014.

[258] S. Pittaccio, S. Viscuso, M. Rossini, L. Magoni, S. Pirovano, E. Villa, S. Besseghini, and F. Molteni, "SHADE: A shape-memory-activated device promoting ankle dorsiflexion," *J. Mater. Eng. Perform.*, vol. 18, no. 5-6, pp. 824–830, 2009.

[259] S. S. Cheng, Y. Kim, and J. P. Desai, "Modeling and characterization of shape memory alloy springs with water cooling strategy in a neurosurgical robot," *J. Intell. Mater. Syst. Struct.*, p. 1045389X16685443, 2017.

[260] J. Zhang, E. Merced, N. Sepulveda, and X. Tan, "Optimal compression of generalized Prandtl-Ishlinskii hysteresis models," *Automatica*, vol. 57, pp. 170–179, 2015.

[261] J. Zhang, D. Torres, N. Sepulveda, and X. Tan, "A compressive sensing-based approach for Preisach hysteresis model identification," *Smart Mater. Struct.*, vol. 25, no. 7, 2016.

[262] W. Xu and G. Li, "Constitutive modeling of shape memory polymer based self-healing syntactic foam," *Int. J. Solids Struct.*, vol. 47, no. 9, pp. 1306–1316, 2010.

[263] E. Abrahamson, M. Lake, N. Munshi, and K. Gall, "Shape memory mechanics of an elastic memory composite resin," *J. Intell. Mater. Syst. Struct.*, vol. 14, no. 10, pp. 623–632, 2003.

[264] G. Zhou, H. Zhang, S. Xu, X. Gui, H. Wei, J. Leng, N. Koratkar, and J. Zhong, "Fast triggering of shape memory polymers using an embedded carbon nanotube sponge network," *Sci. Rep.*, vol. 6, 2016.

[265] A. Atalay, V. Sanchez, O. Atalay, D. M. Vogt, F. Haufe, R. J. Wood, and C. J. Walsh, "Batch fabrication of customizable silicone-textile composite capacitive strain sensors for human motion tracking," *Adv. Mater. Technol.*, vol. 2, no. 9, p. 1700136, 2017.

[266] M. Amjadi, M. Turan, C. P. Clementson, and M. Sitti, "Parallel microcracks-based ultrasensitive and highly stretchable strain sensors," *ACS Applied Materials & Interfaces*, vol. 8, no. 8, pp. 5618–5626, 2016.

[267] J. C. Yeo, H. K. Yap, W. Xi, Z. Wang, C.-H. Yeow, and C. T. Lim, "Flexible and stretchable strain sensing actuator for wearable soft robotic applications," *Advanced Materials Technologies*, vol. 1, no. 3, 2016.

[268] J. Sheng and J. P. Desai, "Development of a mesoscale fiberoptic rotation sensor for a torsion actuator," *IEEE Robot. Autom. Lett.*, vol. 3, no. 1, pp. 537–543, 2018.

[269] J. Gafford, H. Aihara, C. Thompson, R. Wood, and C. Walsh, "Distal proprioceptive sensor for motion feedback in endoscope-based modular robotic systems," *IEEE Robot. Autom. Lett.*, vol. 3, no. 1, pp. 171–178, 2018.

[270] Y. Mengüç, N. Correll, R. Kramer, and J. Paik, "Will robots be bodies with brains or brains with bodies?" *Sci. Robot.*, vol. 2, no. 12, 2017.

Jun Zhang is currently an Assistant Professor with the Department of Mechanical Engineering at the University of Nevada, Reno. He received the B.S. degree in Automation from the University of Science and Technology of China, Hefei, China, in 2011, and the Ph.D. degree in Electrical and Computer Engineering from Michigan State University, in 2015. From 2016 to 2018, he was a Post-Doctoral Scholar in Electrical and Computer Engineering at the University of California at San Diego. His current research interests include smart materials, artificial muscles, soft robotics, and assistive robotics.

Jun Sheng is currently a Ph.D. candidate in Robotics in the Wallace H. Coulter Department of Biomedical Engineering at Georgia Institute of Technology. He earned his Bachelor of Science in Mechanical Engineering from Shanghai Jiao Tong University, Shanghai, China, in 2011. He also received his Master of Science in Electrical Engineering from National Taiwan University, Taipei, Taiwan, in 2013. His research interests are centered around surgical robotics, smart actuation and sensing, and biomedical devices.

Ciarán T. O'Neill received his B.A.I and M.A.I in Mechanical and Manufacturing Engineering from Trinity College Dublin, Ireland, in 2013 and 2014, respectively. He is currently a graduate student in Conor Walsh's Group at the Wyss Institute and the School of Engineering and Applied Sciences, Harvard University, USA. His current research interests include wearable robotics, soft robotics and biomechanics.

Conor Walsh received his B.A.I and B.A. degrees in Mechanical and Manufacturing engineering from Trinity College in Dublin, Ireland, in 2003, and M.S. and Ph.D. degrees in Mechanical Engineering from the Massachusetts Institute of Technology in 2006 and 2010. He is currently the John L. Loeb Associate Professor of Engineering and Applied Sciences at the Harvard John A. Paulson School of Engineering and Applied Sciences, a Core Faculty Member of the Wyss Institute for Biologically Inspired Engineering at Harvard, and an Adjunct Associate Professor in the Department of Physical Therapy Athletic Training at Boston University. His current research interests include soft wearable robotics, exoskeletons and human-machine interaction.

Robert J. Wood (F'19) received his M.S. and Ph.D. degrees from the Department of Electrical Engineering and Computer Sciences, University of California, Berkeley, in 2001 and 2004, respectively. He is currently the Charles River Professor of Engineering and Applied Sciences at the Harvard John A. Paulson School of Engineering and Applied Sciences, a Founding Core Faculty Member of the Wyss Institute for Biologically Inspired Engineering at Harvard, and a National Geographic Explorer. His current research interests include microrobotics, soft and wearable robots, and bioinspired robotics.

Jee-Hwan Ryu (M'02) received the B.S. degree in mechanical engineering from Inha University, Incheon, South Korea, in 1995, and the M.S. and Ph.D. degrees in mechanical engineering from the Korea Advanced Institute of Science and Technology, Taejon, South Korea, in 1995 and 2002, respectively. He is currently a Professor with the Department of Mechanical Engineering, Korea University of Technology and Education, Cheonan, South Korea. His research interests include haptics, telerobotics, soft actuators, exoskeletons and autonomous vehicles.

Jaydev P. Desai is currently a Professor and BME Distinguished Faculty Fellow in the Wallace H. Coulter Department of Biomedical Engineering at Georgia Tech. He is also the Director of the Georgia Center for Medical Robotics (GCMR) and the Associate Director of the Institute for Robotics and Intelligent Machines (IRIM). He completed his undergraduate studies from the Indian Institute of Technology, Bombay, India, in 1993. He received his M.A. in Mathematics in 1997, M.S. and Ph.D. in Mechanical Engineering and Applied Mechanics in 1995 and 1998 respectively, all from the University of Pennsylvania. He is a recipient several NIH R01 awards, and NSF CAREER award. He is the Editor-in-Chief of the Journal of Medical Robotics Research and the Encyclopedia of Medical Robotics. His research interests include image-guided surgical robotics, MEMS-based cancer diagnosis, endovascular robotics, and rehabilitation robotics. He is also a fellow of the IEEE, ASME, and AIMBE.

Michael Yip is an Assistant Professor of Electrical and Computer Engineering at UC San Diego and directs the Advanced Robotics and Controls Lab. His research interests include soft robotics for medicine and learning representations for robot control and planning. Yip's work has been recognized through several best paper awards at ICRA, including the 2016 best paper award for IEEE Robotics and Automation Letters. He currently serves as Associate Editor for ICRA and RA-L. He received a B.Sc. in Mechatronics Engineering from the University of Waterloo, an M.S. in Electrical Engineering from the University of British Columbia, and a Ph.D. in Bioengineering from Stanford University. Before UCSD, Yip was a research associate with Disney Research in Los Angeles.